Droughts in western Central Europe and associated atmospheric circulation patterns since 1844

Emile Neimry[1], Hugues Goosse[1], Mathieu Jonard[1]

[1] Earth and Life Institute, Université catholique de Louvain, Louvain-la-Neuve, Belgium

Correspondence to: Emile Neimry (emile.neimry@uclouvain.be)

Abstract. Droughts in western Central Europe have major impacts on agriculture, ecosystems, and society, yet their long-term variability and drivers remain poorly understood. This study investigates drought variability over the past 180 years and its link to atmospheric circulation. Three reanalysis datasets (ERA5, 20CRv3, and ModE-RA), evaluated against long weather station observations, are used to identify meteorological drought events via the 3-month Standardized Precipitation (Evapotranspiration) Indexes (SPI-3 & SPEI-3), and to relate them to atmospheric circulation patterns through k-means clustering of 500 hPa geopotential height anomalies. Results show that recent severe and successive droughts have historical precedents and occur within pronounced multidecadal variability. Yet the 2010s emerge as the driest decade when assessed with SPEI-3, a feature that disappears when only precipitation is considered, highlighting the increasing contribution of atmospheric evaporative demand (AED) to drought severity. Although annual SPEI-3 exhibits no long-term trend, increasing AED has progressively offset increasing precipitation, leading to contrasting seasonal responses with autumn and winter becoming wetter, whereas summer and, more recently, spring becoming drier. Four recurrent circulation patterns associated with droughts in western Central Europe are identified: the Baltic High, British Isles High, North–South Dipole, and European High. Droughts have become increasingly associated with the European High, a pattern characterised by strong anticyclonic anomalies, large positive AED anomalies, and intense droughts, providing a dynamical explanation for the recent emergence of spring drying.

1 Introduction

Drought is a recurring climate phenomenon worldwide, with growing concern in Europe due to the increase in drought events observed over recent decades (Spinoni et al., 2019; Ionita et al., 2020, 2021). Droughts are the most significant environmental hazard in terms of both economic losses (Spinoni et al., 2016; Stahl et al., 2016; Cammalleri et al., 2020; Mens et al., 2022), and human fatalities through famine and disease (Bruce, 1994; Obasi, 1994; Guha-Sapir et al., 2004; Maslin et al., 2025). Both urban and rural environments are highly vulnerable, with particularly severe impacts on agriculture and forest ecosystems (e.g. Choat et al., 2012; Tapia et al., 2017; Vogel et al., 2019).

Despite extensive research, substantial uncertainties remain regarding long-term drought trends. At the global scale, meteorological droughts showed limited evidence of long-term changes since the early to mid-20th century (Sheffield et al., 2012; Spinoni et al., 2014; Vicente-Serrano et al., 2022). Across Europe, drought trends remain difficult to assess because strong multidecadal precipitation variability can obscure long-term signals (Hänsel et al., 2019; Oikonomou et al., 2020). Central Europe represents a particularly uncertain region. Some studies describe this region as a transition zone between drying trends in Southern Europe and wetting trends in Northern Europe since the mid-20th century (Spinoni et al., 2015, 2017, 2018), while others identify Central Europe as part of a broader drying trend (Ionita and Nagavciuc, 2021). While part of the disagreement arises from the differences in spatiotemporal coverage and drought metrics employed (e.g. Freund et al., 2023; compared with Bebchuk et al., 2025), another part originates from the contrasting seasonal responses. While seasonal trends remain sensitive to the definition of the seasons (Hänsel et al., 2019), there is broad agreement that drought conditions intensified during spring and summer across much of Central Europe over the last three to four decades (e.g. Ionita et al., 2020; Philip et al., 2020; Hänsel et al., 2022). In contrast, drought conditions generally weakened during autumn and particularly in winter (e.g. Moberg and Jones, 2005; Hänsel et al., 2009; Spinoni et al., 2017).

Drought variability in Central Europe results from complex interactions between dynamic and thermodynamic processes, whose relative contributions remain uncertain and vary across seasons (van Haren et al., 2013; Suarez-Gutierrez et al., 2020; Hoffmann and Spekat, 2021; Brönnimann et al., 2025). During winter, atmospheric circulation dynamics are hypothesised to dominate, whereas in summer, land–atmosphere feedbacks may play a larger role (Haslinger et al., 2019; Haslinger and Mayer, 2023). Dry conditions over Central Europe are commonly associated with anticyclonic circulation, south-to-easterly winds, and reduced inflow of moist air from the Atlantic (Trnka et al., 2009; Lhotka et al., 2020; Bešťáková et al., 2024). In addition, drought variability has been linked to large-scale circulation features such as the jet stream and teleconnection patterns (e.g. Van Oldenborgh et al., 2000; Brönnimann, 2007; Svensson and Hannaford, 2019; Kim et al., 2023), particularly the North Atlantic Oscillation (NAO) (Hurrell and Van Loon, 1997; Vicente-Serrano and López-Moreno, 2008), even during summer months (Folland et al., 2009; Simpson et al., 2024). Because persistent high-pressure systems simultaneously promote reduced precipitation (Fleig et al., 2011; Kingston et al., 2015; Bakke et al., 2023) and warm extremes (Stefanon et al., 2012; Kautz et al., 2022), the region represents one of the main European hotspots of compound hot and dry events (Ionita et al., 2021), whose impacts exceed those of either hazard occurring in isolation (Zscheischler et al., 2020). Moreover, in a warming climate, the contribution of atmospheric evaporative demand (AED) has become an increasingly important driver of drought severity (Briffa et al., 2009; Gebrechorkos et al., 2025).

Although numerous studies investigated drought variability in Central Europe and its dynamical drivers, western Central Europe—defined here as Belgium, the Netherlands, Luxembourg, northern France, and western Germany—received comparatively limited attention. Yet, this region constitutes one of the major socio-economic centres of Europe (Brunet, 2002), home to approximately 100 million inhabitants in 2020 (WorldPop, 2018), and supports vulnerable ecosystems, including croplands, grasslands, and forests (Zanaga et al., 2022). Given the strong spatial and seasonal variability of drought trends and the influence of multidecadal variability (Hänsel et al., 2019; Vicente-Serrano et al., 2021), this study investigates the evolution of drought conditions and their hydroclimatic drivers in western Central Europe since the pre-industrial era, placing recent droughts in a historical perspective. Moreover, atmospheric circulation has been shown to play a particularly important role in drought variability in western Central Europe compared with many other European regions (Savary et al., 2026; Xue et al., 2026). This study therefore characterises seasonal atmospheric circulation patterns associated with droughts over long time periods, complementing previous work that has mainly focused on specific daily weather types.

2 Methods

2.1 Drought definition

This study focuses on meteorological droughts, given its objective of linking drought events to atmospheric circulation. Drought conditions are characterised using the Standardised Precipitation Index (SPI, McKee et al., 1993), as recommended by the World Meteorological Organization (WMO, 2012), and the Standardised Precipitation Evapotranspiration Index (SPEI, Vicente-Serrano et al., 2010). Both indices transform a fitted distribution of a variable accumulated over a given time scale into a standardised normal distribution ($\mu = 0$, $\sigma = 1$). For SPI, the accumulated variable is precipitation, whereas SPEI is based on the climatic water balance, defined as precipitation minus atmospheric evaporative demand (AED).

AED represents the maximum combined evaporation from soil and transpiration from vegetation under given climatic conditions, assuming no soil water limitation. Although AED is often used interchangeably with potential evapotranspiration (PET), from which the index derives its name, this terminology can be ambiguous and is therefore not recommended (Katerji and Rana, 2011; DeJonge et al., 2025). AED is estimated using the Thornthwaite equation (1948), which does not explicitly parameterise a specific reference surface or vegetation type and requires only temperature and latitude, thereby ensuring methodological consistency across the three datasets. In western Central Europe, this method agrees closely with the more physically-based Penman–Monteith approach (1948). The influence of this approximation on the results is evaluated in the Supplementary Material (Supplementary Evaluation), and its implications are discussed in Section 5.4.

A three-month accumulation period (SPEI-3 and SPI-3) is selected as it is sufficiently long to capture a substantial hydrological imbalance, while remaining short enough to be directly linked to dynamic drivers. The three-month accumulation is calculated using a rolling monthly window, resulting in 12 index values per year. Drought onset occurs when the index falls below -1 (McKee et al., 1993), and drought termination when it rises above this threshold. Drought severity and mean intensity are defined as the sum and mean of the absolute index values during an event, respectively. Drought duration corresponds to the number of consecutive months with index values below -1.

SPI-3 and SPEI-3 are computed using the *SPEI* R package (Beguería et al., 2014). Following Vicente-Serrano et al. (2010) and Stagge et al. (2015), a Gamma distribution is fitted for SPI-3, and a log-logistic distribution for SPEI-3. The indices are computed relative to the 1947–2008 reference period, corresponding to the common period shared by all post-evaluation reanalyses. The indices are computed at both the grid-cell and regional scales. At the regional scale (48°N–54°N, 2°E–10°E), precipitation and AED are aggregated and area-weighted across all land grid cells before the computation of the index to ensure a consistent regional representation, as described in Spinoni et al. (2016). For each month, the drought area involved is also calculated as the proportion of grid cells with index values below -1.

2.2 Atmospheric circulation classification

Because meteorological drivers must persist long enough to trigger drought onset (IPCC, 2013; Raposo et al., 2023), the aim is to relate drought events in western Central Europe to low-frequency atmospheric circulation over the Euro-Atlantic sector (30°N-70°N, 35°W-35°E). The clustering is performed on 500 hPa geopotential height (Z500) anomalies computed relative to the 1947–2008 reference period and focuses on seasonal drought events occurring in February, May, August, and November, corresponding to winter, spring, summer, and autumn, respectively. For each event identified in one of these four months, Z500 anomalies are averaged over that month and the two preceding months (i.e. December–February, March–May, June–August, and September–November, respectively) to match the three-month accumulation period of SPI-3 or SPEI-3. The k-means clustering algorithm of Hartigan and Wong (1979) is then applied to these composites to identify recurrent circulation patterns associated with drought. Separate analyses are performed for SPI-3 and SPEI-3 drought events.

Clustering is performed in the temporal dimension, with grid cells treated as variables and drought-event Z500 composites as observations. As the k-means clustering algorithm minimises the intra-cluster variance, Euclidean distances are weighted by the cosine of the latitude. To assess clustering stability and reduce sensitivity to centroid initialisation (Philipp et al., 2007), the algorithm was repeated 1000 times for each number of clusters between 2 and 20. The dominant patterns remained stable up to six clusters, indicating limited sensitivity to the initial centroid positions.

Prior to clustering, the number of clusters was fixed to four. Monthly-to-seasonal atmospheric circulation is generally characterised by a few broad-scale recurrent patterns (Huth et al., 2008), unlike daily weather-type classifications that typically require more clusters (e.g. Schwander et al., 2017; Pfister et al., 2025). In addition, only drought-related circulation states are considered here, reducing the expected diversity of patterns. Common clustering diagnostics (Fig. S1) suggested between two and six clusters, providing no unique optimum. Four clusters were ultimately selected based on the spatial separability of the resulting patterns.

To characterise the dominant modes of variability and compare them with the different clusters, the first three empirical orthogonal functions (EOFs) are computed from the complete record of seasonal Z500 over the Euro-Atlantic sector, rather than from drought events only. The EOF analysis is performed on seasonal mean Z500 fields weighted by the square root of the cosine of latitude (Chung and Nigam, 1999).

2.3 Trend detection

Temporal trends are detected using the modified Mann–Kendall (MK) test (Mann, 1945; Kendall, 1948) with the variance correction proposed by Hamed and Rao (1998) (hereafter MMKH), implemented through the R package by Patakamuri and O'Brien (2017). The MK test is a non-parametric rank-based method that is widely used for climatological and hydrological time series (Hamed, 2008). Because SPI-3 and SPEI-3 are based on three-month accumulations, they exhibit serial correlation, violating the independence assumption of the MK test. This effect is accounted for using the variance correction of Hamed and Rao (1998), which considers serial correlation across multiple lags (Khaliq et al., 2009) and has been shown to provide good statistical power (Blain, 2013). Trend magnitude is estimated using Sen's slope (Sen, 1968), a non-parametric estimator defined as the median slope between all pairs of observations.

3 Reanalysis datasets and evaluation

Three complementary atmospheric reanalyses are used at monthly resolution, covering different periods, spatial resolutions, and data-assimilation strategies (Table 1). The European Centre of Medium-range Weather Forecasts Reanalysis v.5 (**ERA5**) (Soci et al., 2024) assimilates a broad range of observations, including satellite, aircraft, buoy, ship, surface, and upper-air station data. It provides high-resolution data and extensive variable coverage, although over a shorter period than the other reanalyses. The Twentieth Century Reanalysis version 3 (**20CRv3**) (Slivinski et al., 2019) primarily assimilates surface pressure observations. Its more limited data assimilation provides temporal consistency for long-term climate studies, although with lower accuracy than full-input reanalyses. The Modern Era Reanalysis (**ModE-RA**) (Valler et al., 2024) assimilates proxy records, documentary data, and early instrumental measurements, rendering it particularly useful for analysing multidecadal variability and historical extremes, despite its lower spatial resolution and more limited variable availability.

Table 1: Summary of reanalyses used in this study.

Dataset	References	Type of reanalysis	Data assimilation method	Period covered		Spatiotemporal resolution	
				Original	After evaluation	Original	Resampled
ERA5	Soci et al. (2024)	Full input	4D-Var	1940-2023	1947–2023	0.25° Hourly	0.25° Monthly
20CRv3	Slivinski et al. (2019)	Surface input	Ensemble Kalman Filter	1836-2015	1918–2015	1° 3-hourly	0.25° Monthly
ModE-RA	Valler et al. (2024)	Paleo	Ensemble Square Root Filter	1421-2008	1844–2008	~1.8° Monthly	0.25° Monthly

For spatial comparability, 20CRv3 and ModE-RA were bilinearly interpolated to the ERA5 resolution (0.25° × 0.25°). This interpolation does not introduce additional spatial information but ensures a consistent grid for comparison while preserving the native ERA5 resolution. Therefore, spatial analyses focus on mid- to large-scale structures, as differences below approximately 200 km remain uncertain because of differences in native resolution. At the aggregated regional scale, this resampling has no significant impact on the conclusions. In addition, monthly anomalies from 20CRv3 and ModE-RA were computed relative to their respective climatologies and then multiplied by the corresponding 1979–2008 ERA5 climatology. This adjustment harmonises the datasets while preserving their relative temporal variability. The 1979–2008

ERA5 climatology is used only for this step, as ERA5 is considered the most reliable reanalysis during the recent overlapping period.

Reanalysis reliability depends on model performance, the data assimilation method, and the density and quality of assimilated observations, which generally decrease further back in time. The datasets were therefore evaluated before further analysis. The evaluation compares SPI-3 and SPEI-3 from the reanalyses with long-term station observations at Uccle, De Bilt, Frankfurt am Main, and Paris-Le Bourget (Table S1). These stations were selected from the KNMI Climate Explorer dataset (2022) based on the availability of long, near-continuous temperature and precipitation records. Updated Uccle observations until 2023 and Penman–Monteith AED estimates were obtained from the Royal Meteorological Institute of Belgium. The latter were used to assess the sensitivity of AED estimates to the Thornthwaite method.

The evaluation considers both the general behaviour of the drought indices and the identification of drought events. Index behaviour is assessed using the 10-year left-moving mean absolute error (MAE) between each reanalysis and station record. Drought-event identification is evaluated using the 20-year left-moving Matthews correlation coefficient (MCC, Matthews, 1975), which provides an excellent measure of agreement between binary classifications (Chicco and Jurman, 2020). A period is retained only when both criteria are satisfied across the station network. Specifically, reliable periods require the moving MAE to remain below 0.5 and the moving MCC to remain above 0.4.

SPI-3 provides the clearest constraints on reliable periods and is therefore shown in Fig. 1, while SPEI-3 shows broadly similar behaviour (Fig. S2). After the early 1960s, all reanalyses closely follow the station-based SPI-3 and SPEI-3 variability, and drought-event agreement is generally good, especially at Uccle and De Bilt. Before the 1960s, larger discrepancies appear between datasets. ERA5 shows excessive dryness during the first years of its record, particularly at Frankfurt, likely related to the limited availability of upper-air temperature observations before 1946 (Soci et al., 2024) and therefore their influence on atmospheric water vapour and precipitation over land. 20CRv3 shows excessive wetness before the late 1910s, consistent with the sharp increase in assimilated Northern Hemisphere observations in the early 1920s (Slivinski et al., 2021). ModE-RA performs reliably from 1844 onward, while its lower reliability before the 1840s likely reflects the limited number of assimilated observations.

The retained periods are therefore 1947–2023 for ERA5, 1918–2015 for 20CRv3, and 1844–2008 for ModE-RA, extending the analysis back to the pre-industrial era (IPCC, 2013). In addition, reanalyses show good agreement between themselves in identifying regional drought events, especially between ERA5 and ModE-RA. Over the common reference period, MCC values are 0.46 for ERA5–20CRv3, 0.44 for 20CRv3–ModE-RA, and 0.79 for ERA5–ModE-RA for SPEI-3, with similar values for SPI-3 (0.45, 0.41, and 0.78, respectively).

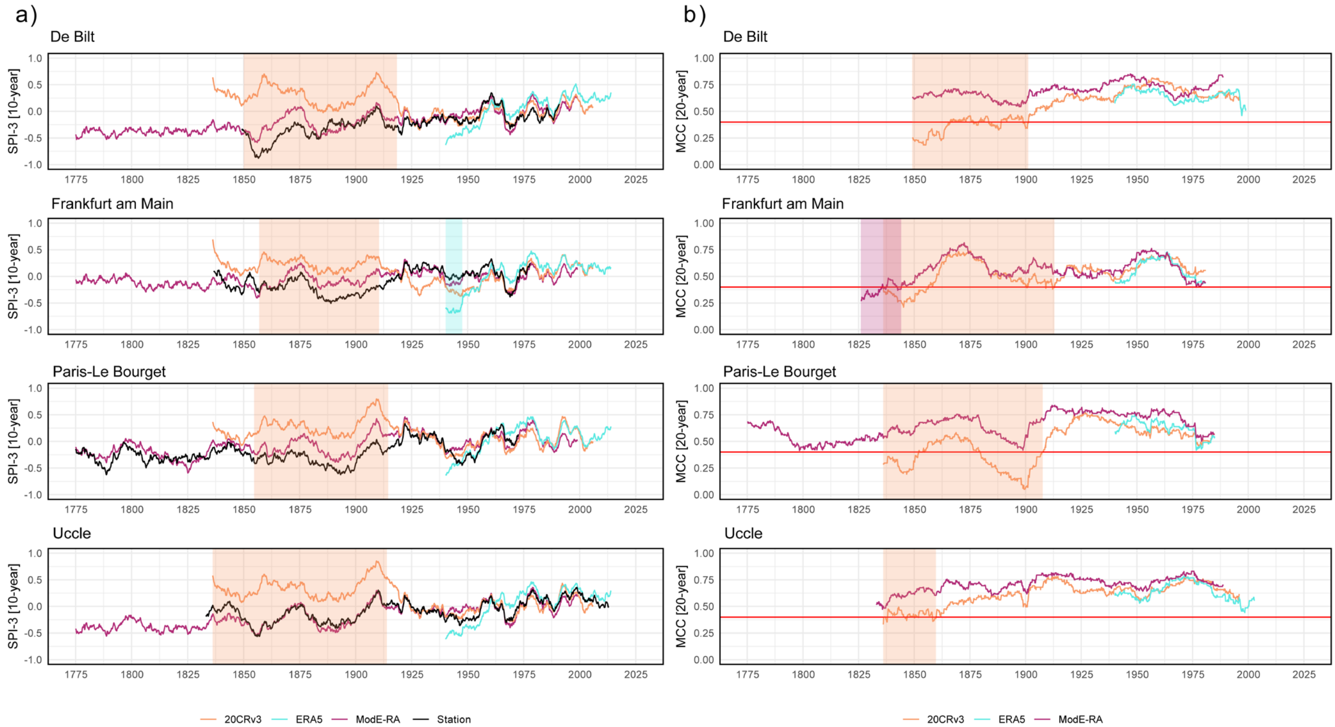

Figure 1: Data evaluation based on (a) the 10-year left-moving average of SPI-3, , calculated using the 1940–2000 evaluation reference period, for each reference station and reanalysis, and (b) the 20-year Matthews correlation coefficient (MCC) for drought classification between each reference station and the reanalyses. For each reanalysis–station pair in (a), the shaded period begins when the 10-year left-moving mean absolute error exceeds 0.5 and extends until it subsequently decreases below 0.5 and remains below this threshold. In (b), the shaded period begins when the 20-year left-moving MCC falls below 0.4 and extends until it subsequently rises above 0.4 and remains above this threshold. In both panels, shaded areas are coloured according to the dataset considered unreliable during the corresponding periods.

4 Results

4.1 Drought events

Regional drought indices (Fig. 2a and Fig. S3a) are strongly correlated with the spatial extent of drought ($r = 0.77$–0.81 for SPEI-3 and 0.81–0.84 for SPI-3), indicating that they provide a representative measure of regional drought conditions. The most severe droughts (Fig. 2a), defined as those exceeding the 90th percentile of drought severity over the 1947–2008 reference period for each reanalysis, affected the entire region at their peak (Fig. 2b and Fig. S3b), demonstrating high spatial coherence across western Central Europe. Among them, the 1921 drought stands out because of its exceptional duration (14 months in ModE-RA), resulting in a severity exceeding twice the 90th percentile threshold for SPEI-3.

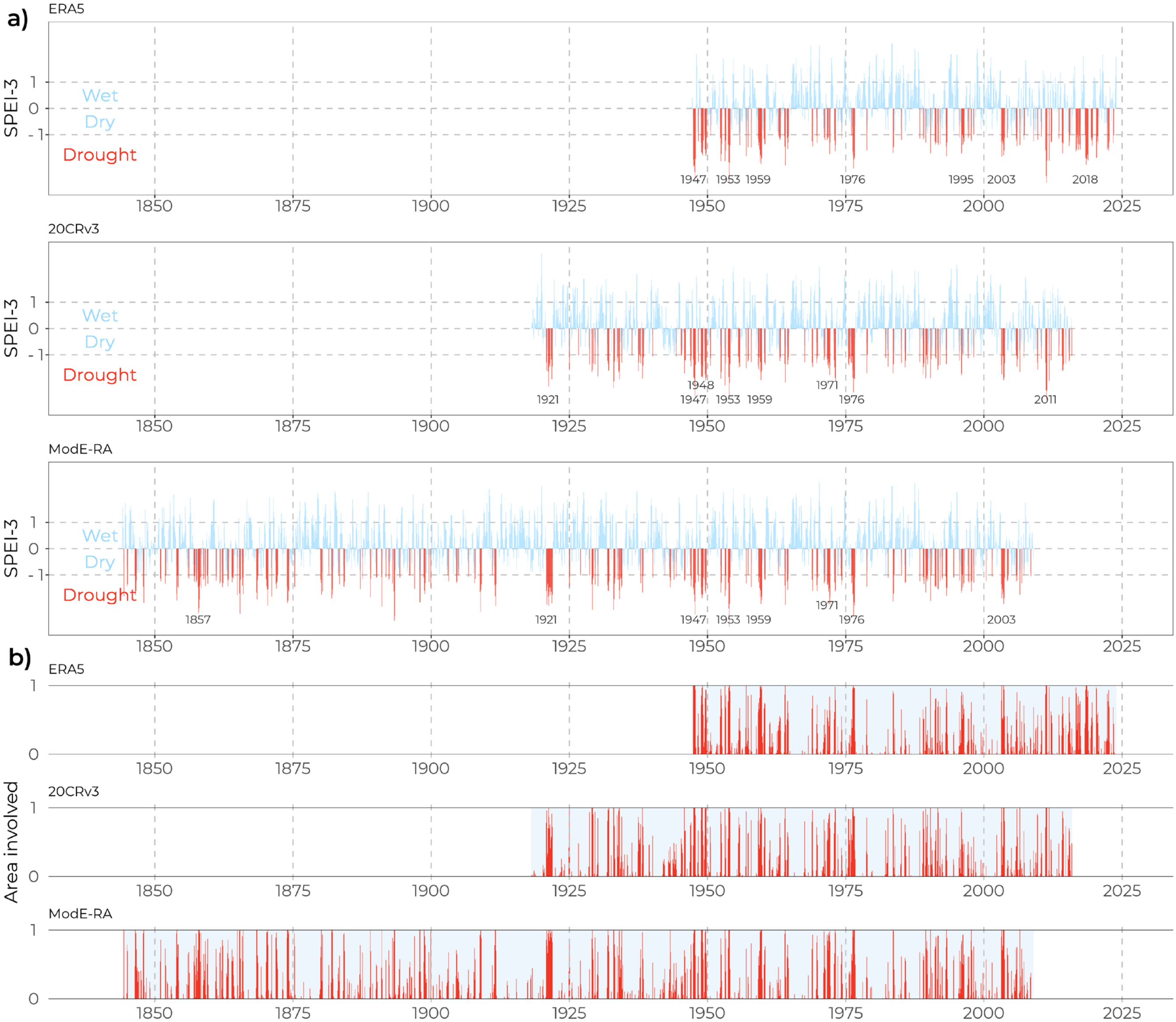

Figure 2: (a) 3-month Standardized Precipitation Evapotranspiration Index time series for the aggregate western Central Europe region for each reanalysis dataset (each row) (reference period: 1947–2008). The red bars indicate drought months (SPEI-3 < -1), and the most severe drought events are highlighted. (b) Time series of the proportion of the western Central Europe region under drought (illustrated in red) according to the SPEI-3 values of the grid cells.

SPI-3 and SPEI-3 identify largely the same drought events (Fig. 2; Fig. S3), with MCC values of 0.76 (ERA5), 0.81 (20CRv3), and 0.74 (ModE-RA) over the common reference period. However, their intensity and severity differ. For example, the well-documented 1976 drought is more intense according to SPI-3, whereas the recent 2018 drought is more intense according to SPEI-3. Since the 1990s, SPEI-3 identifies more droughts, with longer durations than SPI-3 (ERA5, 1990–2023: 33 vs. 25 events, mean duration 2.61 vs. 2.08 months), while mean peak intensity is only slightly higher (1.48 vs. 1.44). Conversely, the most severe droughts are more numerous and generally occur earlier in the record according to SPI-3. In addition to the most severe droughts common to both indices (Fig. 2a and Fig. S3a), the 2003 and 2011 droughts appear for SPEI-3 only, whereas the 1853, 1870, 1873, 1893, 1908, 1911, and 1929 droughts appear only with SPI-3.

The recent period 2011–2023 was characterised by frequent droughts, particularly according to SPEI-3 (29.2 drought months per decade in ERA5). Similar periods also occurred during 1857–1874 (31.7 drought months per decade in ModE-RA) and 1947–1960 (29.3–34.3 drought months per decade depending on the reanalysis). In contrast, drought frequency was particularly low during 1912–1920 (1.6 drought months per decade in ModE-RA) and 1977–1988 (6.7–8.3 drought months per decade).

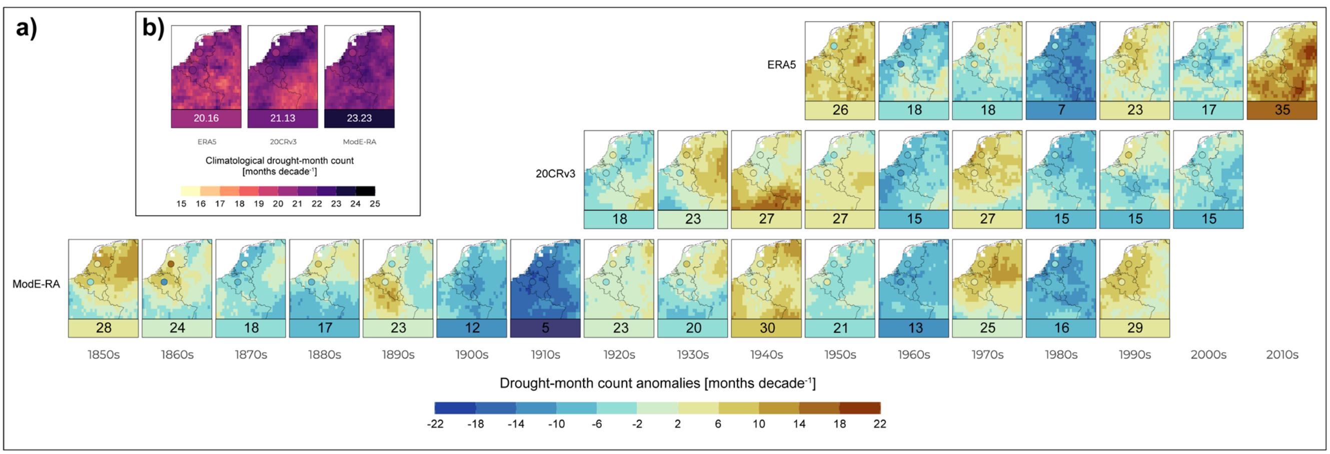

Figure 3: (a) Anomalies in decadal SPEI-3 drought-month counts for each dataset (rows) and complete decade (columns), relative to (b) the mean number of SPEI-3 drought months per decade over the 1947–2008 reference period. Positive values in (a) indicate more drought months than the climatological decadal mean, whereas negative values indicate fewer. The absolute number of drought months computed at the regional scale is shown below each corresponding map. Discs represent anomalies at weather stations that fully cover both the corresponding decade and the reference period.

Decadal drought-month count (Fig. 3a) further highlights the pronounced multidecadal variability of drought occurrence. According to SPEI-3, the 2010s experienced the highest drought-month frequency since the beginning of the pre-industrial period, with 35 drought months (29% of the decade) in ERA5. Western Germany was particularly affected, locally exceeding 40 drought months during the decade. Conversely, the 1910s experienced only five drought months (4%) according to ModE-RA. These values contrast with the climatological frequency of approximately 20–23 drought months per decade (Fig. 3b), close to the 16% expected from the standardised drought threshold (SPI/SPEI < -1). The SPI-3 perspective differs substantially (Fig. S4). In particular, the 2010s no longer emerge as an exceptionally dry decade, exhibiting the largest differences between SPI-3 and SPEI-3.

4.2 Hydroclimatic trends

Year-round SPI-3 and SPEI-3 exhibit contrasting long-term trends (Fig. S5). SPI-3 indicates a long-term wetting over the past 180 years, consistent with increasing 3-month precipitation in all reanalyses (Fig. 4a), with high statistical confidence for ModE-RA and ERA5. In contrast, SPEI-3 exhibits no significant long-term trend, indicating that increasing AED has offset much of the precipitation increase. The strongest increases in both precipitation and AED occur during the most recent period, consistent with accelerated warming. Indeed, their increases per degree of warming are consistent across the three reanalyses (Table S2), despite their different temporal coverage. Warming itself accelerated over time, reaching 0.42 K per decade during 1990–2023 in ERA5.

Seasonal trends reveal a marked contrast between winter and summer. Winter exhibits widespread wetting in both indices, particularly over 1844–2008 (ModE-RA) and 1947–2023 (ERA5), driven by increasing precipitation that outweighs the comparatively small increase in AED, despite substantial warming (Fig. 4a). Conversely, summer shows the strongest increase in AED, which largely offsets increasing precipitation in ERA5 and 20CRv3, resulting in SPEI-3 drying (low statistical confidence, Fig. S5). Over 1844–2008, ModE-RA indicates summer drying because of both increasing AED and decreasing precipitation. However, this pattern is not reproduced by ERA5 or 20CRv3 over their common period with ModE-RA (Fig. S6), nor by the station observations (Fig. S7).

Spring and autumn generally exhibit intermediate behaviour between the winter and summer extremes (Fig. 4a). Over 1844–2008 and 1918–2015, increasing AED offsets precipitation increases, producing little change in SPEI-3. During 1947–2023, spring is more similar to summer, with SPI-3 wetting but SPEI-3 drying (low statistical confidence), whereas autumn closely resembles winter, with wetting in both indices (high statistical confidence for SPI-3, moderate for SPEI-3). However, station observations do not support the autumn wetting, except at De Bilt, while Uccle shows a statistically significant SPEI-3 drying trend (Fig. S8). The seasonal divergence between SPI-3 and SPEI-3 is greatest in spring over 1844–2008, followed by autumn (Fig. S5), indicating a comparatively strong influence of AED despite smaller absolute increases than in summer.

While the previous results describe aggregated regional trends, local analyses reveal spatial variability (Fig. 4b–c). Agreement between reanalyses is lower locally than regionally (Fig. S8), and correspondence with station observations is less consistent. Nevertheless, several spatial features emerge. Year-round local trends broadly follow the regional signal, except for a significant SPEI-3 wetting along the Dutch coast during 1947–2023. Winter exhibits widespread wetting across the region, in agreement with the station observations. In contrast, spring and summer drying patterns vary spatially and reflect both decreasing precipitation and increasing AED, whereas autumn displays relatively homogeneous wetting despite slight SPEI-3 drying at Uccle.

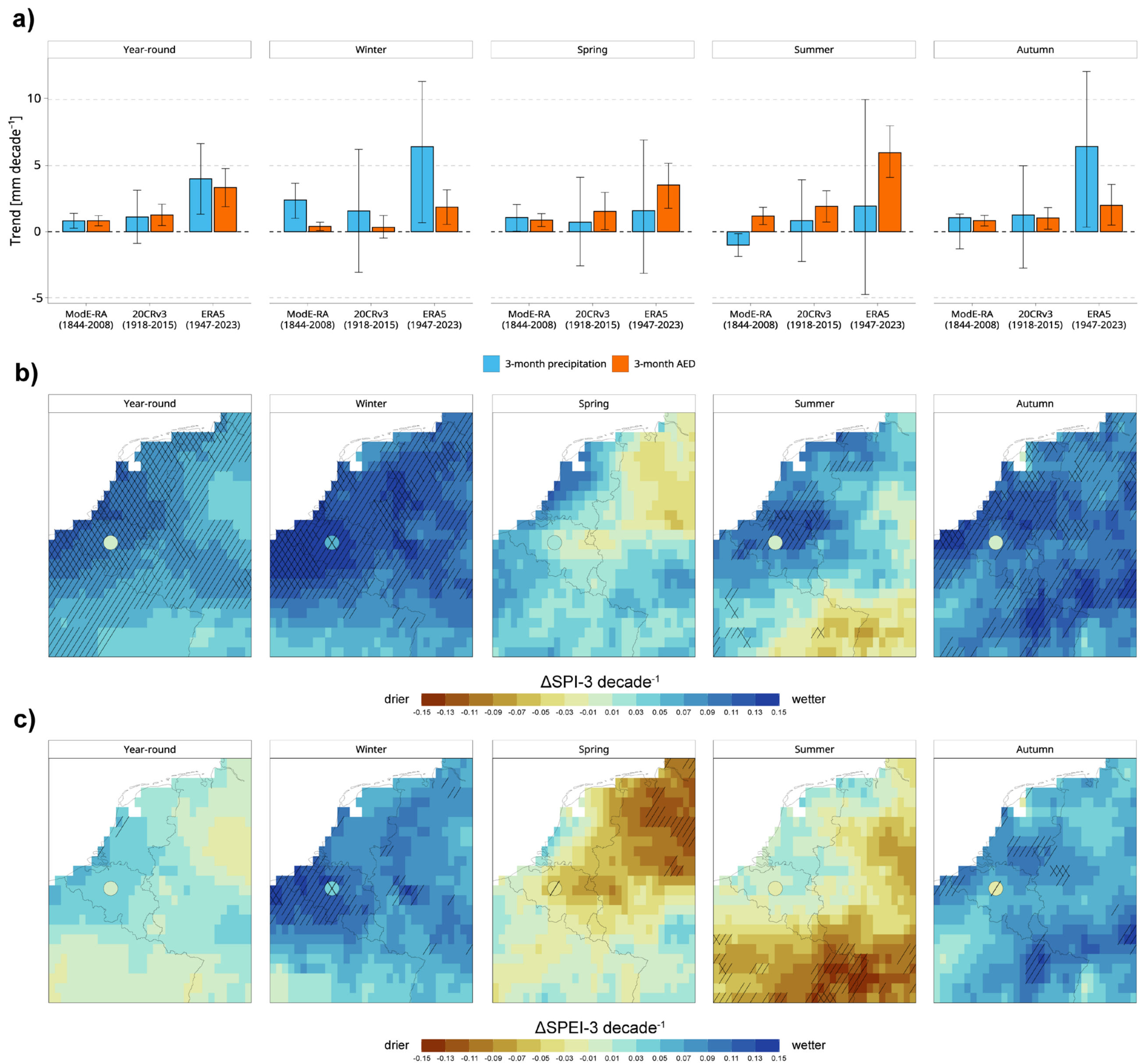

Figure 4: (a) Year-round and seasonal trends per decade in 3-month precipitation and AED for each period–reanalysis combination, estimated using Sen's slope. Error bars indicate the 95% confidence interval of Sen's slope, accounting for the variance correction proposed by Hamed and Rao (2008). Sen's slope maps of year-round and seasonal SPI-3 (b) and SPEI-3 (c) per decade over 1947–2023 (ERA5). Discs represent the Sen's slope of SPEI-3 at the Uccle weather station over the same period, the only station in the datasets used in this study with a continuous record spanning 1947–2023. A single diagonal line indicates a modified Mann–Kendall test *p*-value < 0.05, whereas two crossing diagonal lines indicate *p* < 0.001.

4.3 Atmospheric circulation patterns

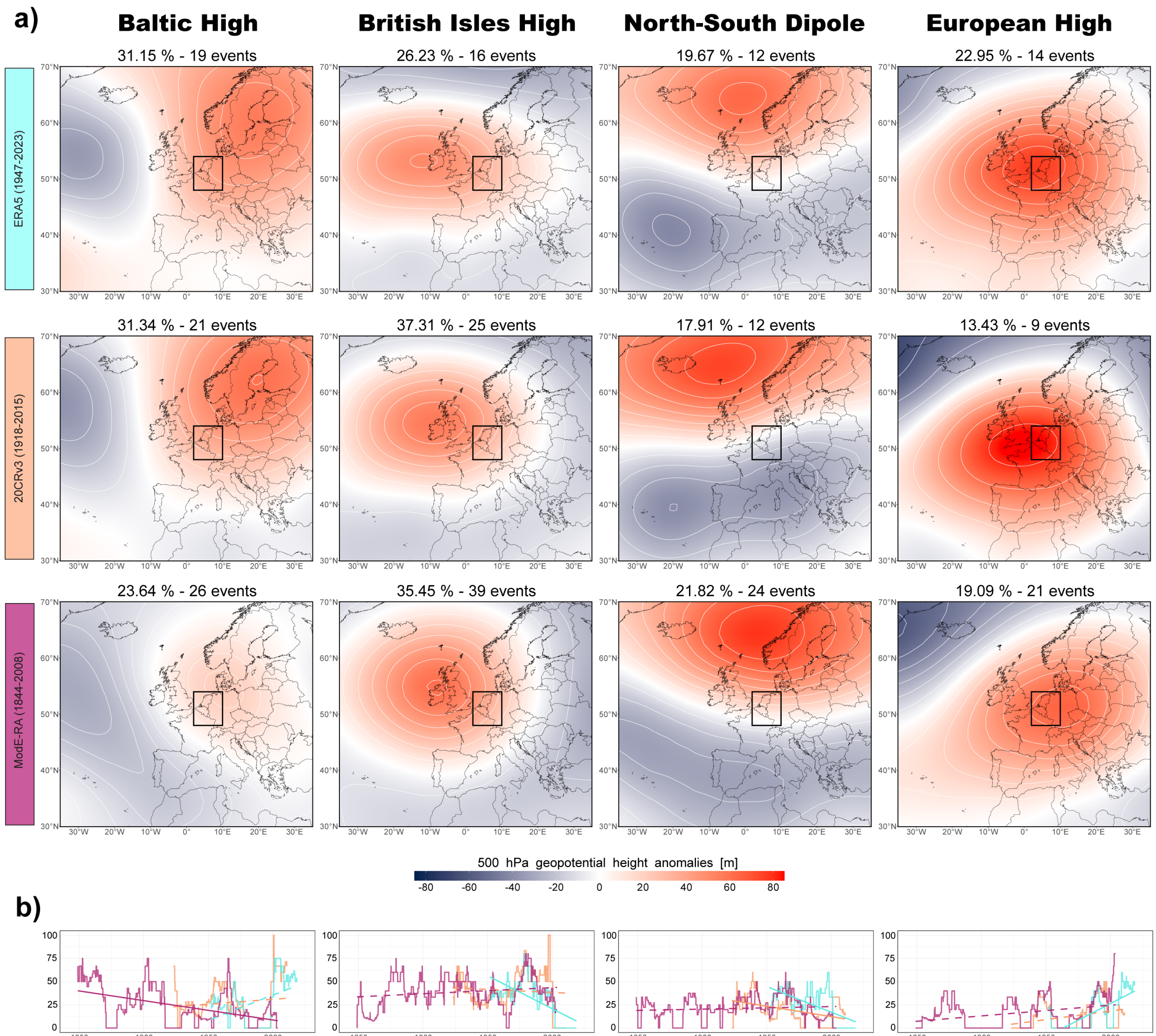

Figure 5: Atmospheric circulation patterns identified from SPEI-3 drought-based clustering (a) and associated drought occurrence trends (b). (a) Cluster centroids of 500 hPa geopotential height anomalies (reference period: 1947–2008) for each period–reanalysis combination. The numbers above each map indicate the percentage and number of drought events assigned to the corresponding cluster within each period–reanalysis combination. The western Central Europe region is delineated by the black box. (b) Ten-year moving fraction (%) of drought events associated with each cluster, using the same colours as in (a).

Straight lines represent linear regressions fitted to the moving fractions. Solid lines indicate statistically significant trends according to the modified Mann–Kendall test ($p < 0.05$), whereas dashed lines indicate non-significant trends ($p \geq 0.05$).

Four atmospheric circulation patterns have been identified from the clustering of Z500 anomalies during drought events defined by SPEI-3 (Fig. 5a) and SPI-3 (Fig. S9a): a high Z500 anomaly centred over the Baltic region; a high Z500 anomaly centred over the British Isles; a dipole of a high Z500 anomaly over Northern Europe and a low Z500 anomaly over Southern Europe; and a high Z500 anomaly centred over the European continent. These patterns are hereafter referred to as Baltic High, British Isles High, North–South Dipole, and European High, respectively. For SPEI-3, the Baltic High is less clearly defined in ModE-RA (1844–2008) than in 20CRv3 (1918–2015) and ERA5 (1947–2023). For SPI-3, the centre of the European High is slightly shifted towards the British Isles in ModE-RA and 20CRv3. The circulation patterns identified over the common reference period (1947–2008) exhibit lower spatial agreement between reanalyses than those identified over their respective full periods, likely because fewer drought events are available to robustly characterise the patterns.

The British Isles High (26–37% of SPEI-3 droughts depending on the reanalyses) and the Baltic High (24–31%) are the most frequent circulation patterns associated with drought, whereas the North–South Dipole and the European High occur less frequently. The Baltic High is more often associated with SPEI-3 droughts than SPI-3 droughts, whereas the opposite is true for the British Isles High (Fig. 5a; Fig. S9a). Over time, droughts have become increasingly associated with the European High in all reanalyses for both indices (moderate to high statistical confidence). An increase in association with the Baltic High is also observed over 1947–2023. Conversely, associations with the British Isles High and the North–South Dipole declined during 1947–2023 in ERA5 (high statistical confidence) (Fig. 5b; Fig. S9b).

The first three dominant modes of variability identified from the EOF analysis correspond to the North Atlantic Oscillation (NAO), the East Atlantic (EA) pattern, and the Scandinavia (SCA) pattern (Barnston and Livezey, 1987; Hernandez and Comas-Bru, 2025; Topál et al., 2025) (Fig. S10). The Baltic High is primarily associated with SCA+ and, to a lesser extent, EA+, whereas the British Isles High is associated with EA−. The North–South Dipole combines SCA+ with NAO−, while the European High is mainly associated with NAO+ over 1844–2008 and 1918–2015 (Fig. 6a; Figs. S11a–S12a).

Winter droughts occur predominantly under the North–South Dipole, spring droughts under the European High, whereas the Baltic High and British Isles High occur throughout the year (Fig. 6b; Figs. S11b–S12b). Autumn droughts are almost exclusively associated with these latter two patterns. In terms of the dominant modes of variability, winter droughts are characterised by EA− and SCA+, summer and autumn droughts by NAO+, whereas spring shows only weak relationships with the dominant modes (Fig. S13).

Droughts associated with the Baltic High and especially the European High exhibit the largest positive AED anomalies, whereas the North–South Dipole is generally characterised by negative AED anomalies (Fig. 6c; Figs. S11c–S12c).

Although the magnitude of precipitation anomalies remains substantially larger than that of AED anomalies, AED anomalies associated with droughts increased over time, whereas precipitation anomalies weakened across all periods, particularly over 1947–2023 (Fig. S14).

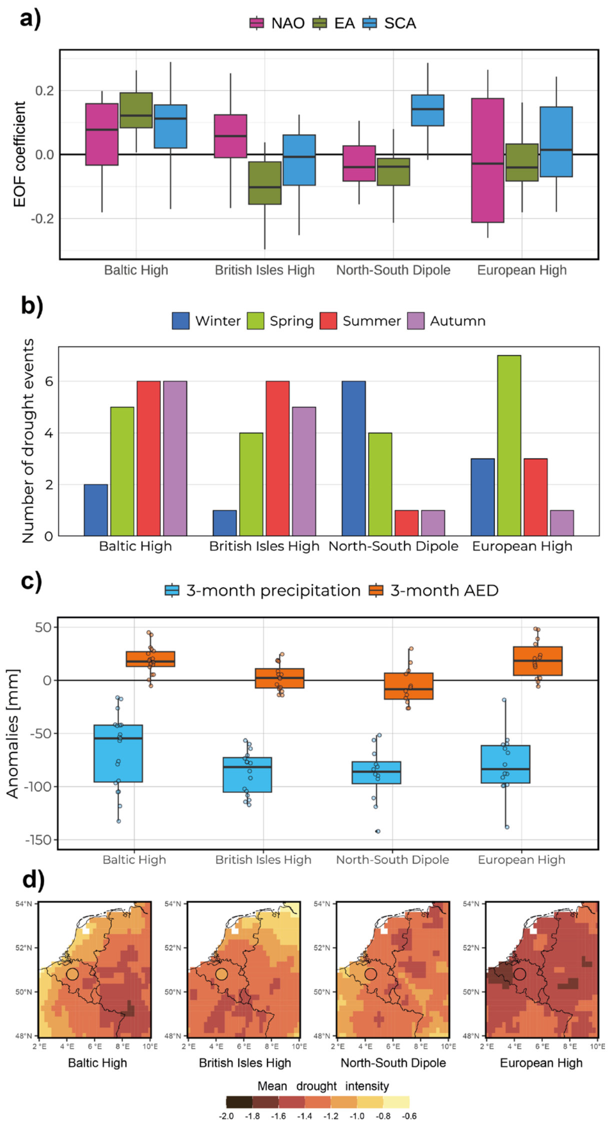

Figure 6: Atmospheric circulation pattern characteristics associated with SPEI-3 drought-based clustering over 1947–2023 (ERA5). (a) Boxplots of EOF coefficients from seasonal EOF analyses of the full Euro-Atlantic record for drought events associated with each circulation pattern (all seasons pooled). (b) Seasonal distribution of drought events for each circulation pattern. (c) Boxplots of 3-month atmospheric evaporative demand (AED) and precipitation anomalies for each cluster, with individual events shown as jittered points. For (a) and (c), the black line indicates the median, the box boundaries represent the

first and third quartiles, and the whiskers extend to the most extreme values within 1.5 times the interquartile range (IQR). Values beyond the whiskers are shown as individual outliers. (d) Maps of the mean SPEI-3 drought intensity for each cluster. Discs represent the mean SPEI-3 drought intensity at the Uccle weather station over the same period, the only station in the datasets used in this study with a continuous record spanning 1947–2023.

Drought intensity also varies with the associated circulation pattern (Fig. 6d; Figs. S11d–S12d). The North–South Dipole is associated with the weakest droughts, particularly over the central and southern parts of western Central Europe. Baltic High events are associated with stronger droughts over the southeastern part of the region, whereas British Isles High events are associated with stronger droughts over the western part. The European High is associated with the most intense SPEI-3 droughts over 1918–2015 and 1947–2023, especially over western Belgium and northern France. This enhancement is much less pronounced for SPI-3 (not shown), consistent with the larger positive AED anomalies associated with the European High.

5 Discussion

5.1 Long perspective on recent events

Recent severe droughts, particularly the 2018 event, have attracted considerable attention (e.g. Bakke et al., 2020; Zscheischler and Fischer, 2020; Huang et al., 2021). However, the present results show that comparable events have occurred previously in western Central Europe, consistent with earlier studies (e.g. Vicente-Serrano et al., 2021). Notably, the 1921 drought (Bonacina, 1923; Briffa et al., 1994; Bertrand et al., 2021) emerges as the most severe event in western Central Europe over 1844–2023 and has likewise been identified among the most severe European droughts of the past centuries (Hanel et al., 2018; van der Schrier et al., 2021). This conclusion nevertheless depends on the metric considered. Based on precipitation alone (SPI-3), the most severe droughts occur predominantly during the earlier part of the record, in agreement with the long-term increase in precipitation. When AED is included (SPEI-3), recent droughts exhibit an increasing potential to reach comparable severity because of the growing contribution of AED to drought severity (Gebrechorkos et al., 2025). In the future, droughts similar to that of 2018 are expected to become even more severe, partly owing to increasing AED (van der Wiel et al., 2021; Aalbers et al., 2023). Moreover, the exceptional severity of the 1921 drought primarily reflects its persistence (14 months in ModE-RA) rather than its peak or mean intensity. During the growing season, more recent droughts (1947, 2003, and 2018) exceed the 1921 event in severity (Hanel et al., 2018; Hänsel, 2020; van der Schrier et al., 2021). Overall, these findings show that recent droughts are not unprecedented but differ from historical events in both their characteristics and underlying drivers, highlighting the importance of combining multiple drought indices (Lloyd-Hughes, 2014).

Beyond individual events, successive dry periods comparable to 2011–2023 occurred during 1857–1874 and 1947–1960, separated by relatively wet intervals during 1912–1920 and 1977–1988. This pronounced multidecadal variability agrees with previous studies (Briffa et al., 1994; van der Schrier et al., 2006; Haslinger et al., 2019; Hänsel et al., 2019; Bertrand et al., 2021). In particular, the 2010s constitute the decade with the highest drought-month frequency over western Central Europe since the 1850s, extending the findings of Lekarkar et al. (2026) for Belgium over the 1970–2020 period. To investigate the drivers of this multidecadal variability, teleconnection indices were examined, but no substantial relationship was found with the NAO, the El Niño–Southern Oscillation, or the Atlantic Multidecadal Oscillation. Although Atlantic SST variability has been linked to Central European drying (e.g. Haslinger et al., 2019; Tuel and Eltahir, 2021; Haslinger and Mayer, 2023), the associated mechanisms remain uncertain. Likewise, although prolonged periods of reduced precipitation and enhanced AED have been shown to favour multi-year droughts over western Central Europe, the underlying processes remain poorly understood (van der Wiel et al., 2023; van Mourik et al., 2025). Given the greater impacts of multi-year droughts compared with shorter droughts (Chen et al., 2025; Hoover and Smith, 2025; Ruijsch et al., 2025) and their expected increase under warmer climate conditions in western Central Europe (van der Wiel et al., 2023), the successive dry periods identified here provide useful case studies for future research.

5.2 Changing contribution of atmospheric evaporative demand

Because precipitation predominantly influences SPEI-3 in the relatively humid climate of western Central Europe (Raible et al., 2017; Tomas-Burguera et al., 2020), the contribution of AED to drought events was expected to be minor. However, although increasing AED has been offset by increasing precipitation, resulting in no long-term trend in SPEI-3, drought events have become increasingly characterised by larger AED anomalies relative to precipitation anomalies. In ERA5, this is reflected in seasonal drought events since 1990, which exhibit larger mean AED anomalies (24.3 vs. 7.3 mm) and less negative mean precipitation anomalies (−59.7 vs. −81.2 mm) than those during 1947–1989. Consequently, although negative precipitation anomalies remain the primary driver of droughts, the contribution of AED has increased markedly over time, making AED a substantial contributor to drought severity. This increasing contribution of AED reflects both the reduction in negative precipitation anomalies caused by increasing precipitation and the intensification of AED anomalies under warming. Since the 1990s, western Central Europe has warmed at 0.42 K per decade (ERA5), exceeding the global mean warming rate (e.g. Dong et al., 2017; Yin et al., 2024; Douville et al., 2025) and making the region particularly sensitive to AED (Huang et al., 2021; Wang et al., 2025). Recent droughts have therefore been increasingly amplified by warming, whereas earlier droughts were primarily associated with larger negative precipitation anomalies. This shift is illustrated by the 2010s, which no longer emerge as an exceptionally dry decade when AED is neglected. These findings therefore highlight the importance of systematically accounting for AED in drought monitoring, particularly from the 1990s onwards.

The relative influence of precipitation and AED differs when considering background hydroclimatic trends rather than individual drought events. At the annual scale, the opposing effects of precipitation and AED on the climatic water balance remain broadly balanced because both variables have increased by comparable magnitudes. Seasonally, however, contrasting responses emerge. The growing divergence between SPI-3 and SPEI-3 reflects the increasing contribution of AED but is not solely controlled by absolute AED trends. Because both indices are standardised, it also depends on the seasonal variability of the climatic water balance. Consequently, despite smaller absolute increases in AED than in summer, spring and autumn exhibit the largest increase in the relative contribution of AED over 1844–2008 (3-month AED increase: 14.5 and 13.8 mm in spring and autumn, respectively, compared with 19.5 mm in summer; SPI-3 − SPEI-3 divergence: 0.41 and 0.31, compared with 0.26 in summer). During the more recent periods, however, the much larger increase in AED made summer the season with the largest contribution of AED to SPEI-3 trends, whereas winter showed the smallest because of lower temperatures. Nevertheless, winter displays the largest proportional increase in AED (33% K^{-1} in ERA5), reflecting the strong energy limitation of winter evapotranspiration. Accordingly, winter and autumn became wetter because large precipitation increases exceeded those in AED, whereas summer and, during recent decades, spring experienced drying because large warming-driven increases in AED outweighed the more limited precipitation gains.

5.3 Atmospheric circulation and drought evolution

The four circulation patterns identified in this study represent distinct hydroclimatic environments over western Central Europe. The Baltic High and the European High are associated with the largest positive AED anomalies, whereas the British Isles High is characterised primarily by negative precipitation anomalies and the North–South Dipole by winter precipitation anomalies combined with negative AED anomalies. These differences reflect the associated flow. The Baltic High induces southeasterly circulation, transporting warm continental air (Serras et al., 2024) that enhances AED, explaining why droughts associated with this pattern are more frequently identified by SPEI-3 than SPI-3. Conversely, the British Isles High favours cooler northerly flow, in line with its association with EA− and the positive relationship between the EA pattern and temperature (Hernandez and Comas-Bru, 2025), resulting in near-zero AED anomalies. The large negative precipitation anomalies associated with this pattern may arise because moist air precipitates over the Scandinavian mountains, leaving western Central Europe in the rain shadow (Pauling et al., 2006). The North–South Dipole occurs predominantly during winter and is associated with SCA+ and NAO−, both linked with cold and dry winter conditions (Bladé et al., 2012; Simpson et al., 2024; Hernandez and Comas-Bru, 2025). This explains its negative AED anomalies, as easterly continental air masses are colder than maritime air masses during winter (Stahl and Demuth, 1999), and consequently why droughts associated with this pattern are generally the weakest. Consistent with the tendency for drought intensity in western Central Europe to increase closest to the largest positive Z500 anomalies (Kingston et al., 2015; Bakke et al., 2023), the European High combines strong negative precipitation anomalies with the largest positive AED anomalies. This agrees with previous studies linking persistent anticyclonic circulation to compound hot (Stefanon et al., 2012; Kautz et al., 2022) and dry (Lhotka et al., 2020; Savary et al., 2026) events through large-scale subsidence, reduced cloud cover and enhanced incoming shortwave radiation.

While the year-round precipitation trends (6–8% K^{-1}, Table S2) are broadly consistent with expected Clausius–Clapeyron thermodynamic scaling (~7% K^{-1}), the contrasting seasonal trends highlight the role of atmospheric circulation.

The evolving association of droughts with these circulation patterns provides a coherent interpretation of the seasonal hydroclimatic evolution, particularly during winter and spring. Winter wetting, characterised by particularly large precipitation increases (12–18% K^{-1}), is consistent with the declining association of droughts with the North–South Dipole, the dominant circulation pattern for winter droughts. Because this pattern is closely linked with NAO−, the observed shift towards more positive winter NAO phases since the mid-twentieth century (Visbeck et al., 2001; Hasanean et al., 2023) provides a plausible explanation for the large increase in winter precipitation, in agreement with the established positive relationship between winter NAO and precipitation over the study area (Simpson et al., 2024). Conversely, spring precipitation increased only weakly over 1947–2023 (3.5% K^{-1}), well below the Clausius–Clapeyron scaling, whereas AED increased by more than twice as much. This evolution coincides with the increasing association of droughts with the European High, which predominantly characterises spring droughts. Persistent anticyclonic circulation and blocking have repeatedly been identified as the principal drivers of recent spring droughts in Central Europe (Trnka et al., 2009; Ionita et al., 2015; Lhotka et al., 2020; Bakke et al., 2023; Bešťáková et al., 2024), supporting the circulation changes identified here.

The increasing association of droughts with the European High suggests that compound hot and dry events may become increasingly characteristic feature of droughts in western Central Europe, in agreement with the growing influence of AED identified in this study. This does not imply, however, that circulation patterns primarily associated with negative precipitation anomalies, such as the British Isles High, will become less relevant under a warmer climate, as negative precipitation anomalies remain a necessary condition for drought development and similar circulation patterns have also been projected to become more frequent (Rousi et al., 2021; Tuel and Eltahir, 2021).

5.4 Strengths and limitations

An important strength of this study is the combined use of three independent century-scale reanalyses, each relying on different numerical models, data assimilation systems and assimilated observations. Cross-validation of multiple reanalyses has been recommended to strengthen confidence in analyses of historical climate variability and extreme events (Slivinski, 2018), while reanalyses provide a suitable framework for jointly analysing hydroclimatic variability and atmospheric circulation (Baatz et al., 2021). Evaluation against long weather station observations, together with the comparison over the common reference period, increases confidence in the drought indices. Despite differences between datasets, the principal conclusions regarding drought identification, hydroclimatic trends and atmospheric circulation are consistently reproduced. Remaining discrepancies mainly concern local and seasonal features, reflecting the greater uncertainty of historical precipitation fields and the coarser spatial resolution of reanalyses.

The use of long reanalysis records also highlights the importance of multidecadal variability when interpreting hydroclimatic trends. Sensitivity analyses (not shown) indicate that long-term trends are statistically more robust than trends estimated over recent decades, which are more strongly influenced by the phase of internal climate variability (Hänsel et al., 2019). Consequently, differences between reanalyses primarily reflect their differing temporal coverage rather than contradictory hydroclimatic behaviour. The common reference period provides a practical measure of agreement between datasets, although its relatively short duration is itself influenced by multidecadal variability and should therefore be interpreted with caution. Confidence is highest where datasets converge and lower where agreement across reanalyses or with station observations is limited, such as for the decrease in summer precipitation in ModE-RA and the long-term autumn wetting.

Using both SPI-3 and SPEI-3 additionally strengthens the interpretation by separating the respective roles of precipitation and AED (Lloyd-Hughes, 2014). This interpretation nevertheless depends on the estimation of AED. The temperature-based Thornthwaite formulation can overestimate warming-driven increases in AED (Seneviratne, 2012; Sheffield et al., 2012), consistent with the supplementary evaluation (Supplementary Material). However, these differences do not alter the conclusions regarding drought events, long-term trends, or atmospheric circulation. While Penman–Monteith is more physically based, its homogeneous application across the three reanalyses is precluded by the availability and differing estimation of the required meteorological variables (Córdova et al., 2015), and the additional long-term variables introduce their own uncertainties (Trenberth et al., 2014). More generally, the interpretation of long-term AED changes remains complicated by substantial land-use change and rising atmospheric CO_2 concentrations, which are not explicitly represented by either formulation (Villani et al., 2026). Thus, while AED estimation remains a source of uncertainty, its influence on the regional-scale conclusions appears limited, with the evaluation indicating greater uncertainty in long-term precipitation estimates than that arising from the choice of AED formulation.

The identified seasonal circulation patterns are physically meaningful and consistent with previous classifications of Central European drought weather types at daily timescales (e.g. Stahl and Demuth, 1999; Lhotka et al., 2020; Savary et al., 2026). The seasonal framework adopted here accounts for the pronounced seasonality of atmospheric circulation (Comas-Bru and Hernández, 2018), but splits prolonged droughts spanning multiple seasons into distinct events, particularly during the warm season when droughts are generally longer (Banfi et al., 2024). Seasonal mean circulation patterns may also mask important subseasonal variability. In addition, this approach does not directly quantify changes in the frequency or persistence of circulation patterns, although it successfully captures the recent spring drying, winter wetting, and the associated drought characteristics. However, the circulation patterns alone do not fully explain all aspects of the observed hydroclimatic evolution. In particular, the present framework does not explicitly resolve the respective roles of moisture transport, atmospheric convergence, cloud cover, radiative forcing, and land–atmosphere interactions in drought development. Summer drying and some local features indicate that additional processes may also be important. For example, summer drought evolution is likely influenced by land–atmosphere feedbacks (Seneviratne et al., 2006; Miralles et al., 2019; Suarez-Gutierrez et al., 2020), potentially reinforced by spring drying through soil–moisture preconditioning (Stegehuis et al., 2021; Douville et al., 2025), while the coastal wetting is likely enhanced by increasing North Sea SSTs (Lenderink et al., 2009; Philip et al., 2020). Quantifying the respective contributions of dynamical and thermodynamical processes, particularly during the warm season, remains an important avenue for future research.

6 Conclusion

This study presents the evolution of meteorological droughts in western Central Europe and their associated atmospheric circulation from the mid-19th century to the present, using three complementary reanalysis datasets evaluated against long weather station observations. The combined analysis of SPI-3 and SPEI-3 provides a long-term perspective on recent droughts while disentangling the respective roles of precipitation and AED, whereas the characterisation of seasonal atmospheric circulation patterns further places these hydroclimatic changes into a dynamical framework.

The results show that recent droughts are not unprecedented in terms of severity, with the 1921 drought emerging as the most severe event over 1844–2023 in western Central Europe. The analysis also reveals pronounced multidecadal variability, with successive dry periods (e.g. 1947–1960) repeatedly alternating with markedly wetter intervals (e.g. 1912–1920) over the last 180 years. Furthermore, while the 2010s represent the driest decade since the mid-nineteenth century when AED is considered, analyses based solely on precipitation no longer identify this decade as exceptional, demonstrating the increasing contribution of AED to drought severity under warming, particularly since the 1990s.

Although annual SPEI-3 exhibits no significant long-term trend, this apparent stability masks substantial hydroclimatic changes. Increasing precipitation has compensated for increasing AED at the annual scale, whereas contrasting seasonal responses have emerged. Winter and autumn became wetter as precipitation increases exceeded those in AED, while summer and, more recently, spring experienced drying because warming-driven increases in AED outweighed comparatively limited precipitation gains.

Through k-means clustering of Euro-Atlantic geopotential height anomalies, four atmospheric circulation patterns associated with droughts have been identified: the Baltic High, British Isles High, North–South Dipole, and European High. Their distinct hydroclimatic signatures explain differences in drought intensity and the relative importance of precipitation and AED. The evolving association of droughts with these patterns also provides a coherent interpretation of the observed seasonal hydroclimatic trends, particularly the decline of winter droughts associated with the North–South Dipole and the emergence of spring droughts associated with the European High. This circulation pattern is characterised by strong anticyclonic anomalies over Central Europe and particularly large positive AED anomalies, suggesting that compound hot and dry events may become an increasingly characteristic feature of droughts in western Central Europe.

Overall, these results demonstrate that drought evolution in western Central Europe reflects the interconnected influences of atmospheric circulation, precipitation, atmospheric evaporative demand, and multidecadal hydroclimatic variability. Considering these processes together is therefore essential for placing recent droughts into a long-term perspective and for improving drought monitoring and future risk assessment in a warming climate.

Data and code availability. The reanalyses datasets and the weather station data used in this study are all available online: ERA5 from the Copernicus Climate Change Service implemented by the ECMWF at https://cds.climate.copernicus.eu/; 20CRv3 from the NOAA PSL, Boulder, Colorado, USA, at https://psl.noaa.gov; ModE-RA from Valler et al. (2023) at https://doi.org/10.26050/WDCC/ModE-RA_s14203-18501; Paris, De Bilt and Frankfurt am Main weather station data from the KNMI Climate Explorer at https://climexp.knmi.nl/; Uccle weather station data from the Royal Meteorological Institute of Belgium at https://opendata.meteo.be/. The code and the main diagnostics from this study will be made available upon publication, including SPI-3 and SPEI-3 over western Central Europe for ERA5, 20CRv3, and ModE-RA, as well as atmospheric circulation patterns associated with drought events for the same datasets.

Author contribution. EN: conceptualization; data curation; formal analysis; visualization, writing – original draft and editing. HG & MJ: conceptualization; supervision; writing – review and editing.

Competing interests. The authors declare that they have no conflict of interest.

Acknowledgements. Computational resources have been provided by the supercomputing facilities of the Université catholique de Louvain (CISM/UCL) and the Consortium des Équipements de Calcul Intensif en Fédération Wallonie Bruxelles (CÉCI) funded by the F.R.S.-FNRS under convention 2.5020.11 and by the Walloon Region. Specifically, the R software (R Core Team, 2021) was utilised for the data analysis. GitHub Copilot assisted with coding, while DeepL Write and OpenAI helped with rephrasing sentences. HG is a Research Director within the F.R.S.-FNRS (Belgium). The authors are grateful to Q. Dalaiden and A. Hoy for the constructive discussions.

References

Aalbers, E. E., van Meijgaard, E., Lenderink, G., de Vries, H., and van den Hurk, B. J. J. M.: The 2018 west-central European drought projected in a warmer climate: how much drier can it get?, Nat. Hazards Earth Syst. Sci., 23, 1921–1946, https://doi.org/10.5194/nhess-23-1921-2023, 2023.

Baatz, R., Hendricks Franssen, H. J., Euskirchen, E., Sihi, D., Dietze, M., Ciavatta, S., Fennel, K., Beck, H., De Lannoy, G., Pauwels, V. R. N., Raiho, A., Montzka, C., Williams, M., Mishra, U., Poppe, C., Zacharias, S., Lausch, A., Samaniego, L., Van Looy, K., Bogena, H., Adamescu, M., Mirtl, M., Fox, A., Goergen, K., Naz, B. S., Zeng, Y., and Vereecken, H.: Reanalysis in Earth System Science: Toward Terrestrial Ecosystem Reanalysis, Rev. Geophys., 59, e2020RG000715, https://doi.org/10.1029/2020RG000715, 2021.

Bakke, S. J., Ionita, M., and Tallaksen, L. M.: The 2018 northern European hydrological drought and its drivers in a historical perspective, Hydrometeorology/Mathematical applications, https://doi.org/10.5194/hess-2020-239, 2020.

Bakke, S. J., Ionita, M., and Tallaksen, L. M.: Recent European drying and its link to prevailing large-scale atmospheric patterns, Sci Rep, 13, 21921, https://doi.org/10.1038/s41598-023-48861-4, 2023.

Banfi, F., Cammalleri, C., and Michele, C. D.: A joint spatio-temporal characterization of the major meteorological droughts in Europe, Environ. Res. Lett., 19, 094041, https://doi.org/10.1088/1748-9326/ad6ba9, 2024.

Barnston, A. G. and Livezey, R. E.: Classification, Seasonality and Persistence of Low-Frequency Atmospheric Circulation Patterns, Mon. Weather Rev., 115, 1083–1126, https://doi.org/10.1175/1520-0493(1987)115%3C1083:CSAPOL%3E2.0.CO;2, 1987.

Bebchuk, T., Moir, A. K., Arosio, T., Kirdyanov, A. V., Torbenson, M. C. A., Krusic, P. J., Hindson, T. R., Howard, H., Buchwal, A., Norman, C. A. P., and Büntgen, U.: Taxus tree-ring chronologies from southern England reveal western European hydroclimate changes over the past three centuries, Clim. Dyn., 63, 108, https://doi.org/10.1007/s00382-025-07601-2, 2025.

Beguería, S., Vicente-Serrano, S. M., Reig, F., and Latorre, B.: Standardized precipitation evapotranspiration index (SPEI) revisited: parameter fitting, evapotranspiration models, tools, datasets and drought monitoring, Int. J. Climatol., 34, 3001–3023, https://doi.org/10.1002/joc.3887, 2014.

Bertrand, C., Ingels, R., and Journée, M.: Homogenization and trends analysis of the Belgian historical precipitation time series, Int. J. Climatol., 41, 5277–5294, https://doi.org/10.1002/joc.7129, 2021.

Bešťáková, Z., Kyselý, J., Lhotka, O., Heilig, M., and Eitzinger, J.: Warm-Season Drying Across Europe and Its Links to Atmospheric Circulation, Earth Space Sci., 11, e2023EA003434, https://doi.org/10.1029/2023EA003434, 2024.

Bladé, I., Liebmann, B., Fortuny, D., and van Oldenborgh, G. J.: Observed and simulated impacts of the summer NAO in Europe: implications for projected drying in the Mediterranean region, Clim. Dyn., 39, 709–727, https://doi.org/10.1007/s00382-011-1195-x, 2012.

Blain, G. C.: The modified Mann-Kendall test: on the performance of three variance correction approaches, Bragantia, 72, 416–425, https://doi.org/10.1590/brag.2013.045, 2013.

Bonacina, L. C. W.: The European Drought of 1921, Nature, 112, 488–489, https://doi.org/10.1038/112488b0, 1923.

Briffa, K. R., Jones, P. D., and Hulme, M.: Summer moisture variability across Europe, 1892–1991: An analysis based on the palmer drought severity index, Int. J. Climatol., 14, 475–506, https://doi.org/10.1002/joc.3370140502, 1994.

Briffa, K. R., Van Der Schrier, G., and Jones, P. D.: Wet and dry summers in Europe since 1750: evidence of increasing drought, Int. J. Climatol., 29, 1894–1905, https://doi.org/10.1002/joc.1836, 2009.

Brönnimann, S.: Impact of El Niño–Southern Oscillation on European climate, Rev. Geophys., 45, https://doi.org/10.1029/2006RG000199, 2007.

Brönnimann, S., Franke, J., Valler, V., Hand, R., Samakinwa, E., Lundstad, E., Burgdorf, A.-M., Lipfert, L., Pfister, L., Imfeld, N., and Rohrer, M.: Past hydroclimate extremes in Europe driven by Atlantic jet stream and recurrent weather patterns, Nat. Geosci., 18, 246–253, https://doi.org/10.1038/s41561-025-01654-y, 2025.

Bruce, J. P.: Natural Disaster Reduction and Global Change, Bull. Am. Meteorol. Soc., 75, 1831–1836, https://doi.org/10.1175/1520-0477(1994)075%3C1831:NDRAGC%3E2.0.CO;2, 1994.

Brunet, R.: Lignes de force de l’espace européen, https://doi.org/10.3406/mappe.2002.1759, 2002.

Cammalleri, C., Naumann, G., Mentaschi, L., Formetta, G., Forzieri, G., Gosling, S., Bisselink, B., De, R. A., and Feyen, L.: Global warming and drought impacts in the EU, https://doi.org/10.2760/597045, 2020.

Chen, L., Brun, P., Buri, P., Fatichi, S., Gessler, A., McCarthy, M. J., Pellicciotti, F., Stocker, B., and Karger, D. N.: Global increase in the occurrence and impact of multiyear droughts, Science, 387, 278–284, https://doi.org/10.1126/science.ado4245, 2025.

Chicco, D. and Jurman, G.: The advantages of the Matthews correlation coefficient (MCC) over F1 score and accuracy in binary classification evaluation, BMC Genomics, 21, 6, https://doi.org/10.1186/s12864-019-6413-7, 2020.

Choat, B., Jansen, S., Brodribb, T. J., Cochard, H., Delzon, S., Bhaskar, R., Bucci, S. J., Feild, T. S., Gleason, S. M., Hacke, U. G., Jacobsen, A. L., Lens, F., Maherali, H., Martínez-Vilalta, J., Mayr, S., Mencuccini, M., Mitchell, P. J., Nardini, A., Pittermann, J., Pratt, R. B., Sperry, J. S., Westoby, M., Wright, I. J., and Zanne, A. E.: Global convergence in the vulnerability of forests to drought, Nature, 491, 752–755, https://doi.org/10.1038/nature11688, 2012.

Chung, C. and Nigam, S.: Weighting of geophysical data in Principal Component Analysis, J. Geophys. Res. Atmos., 104, 16925–16928, https://doi.org/10.1029/1999JD900234, 1999.

Comas-Bru, L. and Hernández, A.: Reconciling North Atlantic climate modes: revised monthly indices for the East Atlantic and the Scandinavian patterns beyond the 20th century, Earth Syst. Sci. Data, 10, 2329–2344, https://doi.org/10.5194/essd-10-2329-2018, 2018.

Córdova, M., Carrillo-Rojas, G., Crespo, P., Wilcox, B., and Célleri, R.: Evaluation of the Penman-Monteith (FAO 56 PM) Method for Calculating Reference Evapotranspiration Using Limited Data, Mt. Res. Dev., 35, 230–239, https://doi.org/10.1659/MRD-JOURNAL-D-14-0024.1, 2015.

DeJonge, K. E. and W. R., Allen, K., and et al.: Evapotranspiration Terminology and Definitions, J. Irrig. Drain. Eng., 151, 06025003, https://doi.org/10.1061/JIDEDH.IRENG-10491, 2025.

Dong, B., Sutton, R. T., and Shaffrey, L.: Understanding the rapid summer warming and changes in temperature extremes since the mid-1990s over Western Europe, Clim. Dyn., 48, 1537–1554, https://doi.org/10.1007/s00382-016-3158-8, 2017.

Douville, H., Roehrig, R., and Nabat, P.: Contribution of large-scale atmospheric circulation and anthropogenic aerosols to recent summer warming over western Europe, Clim. Dyn., 63, 208, https://doi.org/10.1007/s00382-025-07689-6, 2025.

Fleig, A. K., Tallaksen, L. M., Hisdal, H., and Hannah, D. M.: Regional hydrological drought in north-western Europe: linking a new Regional Drought Area Index with weather types, Hydrol. Process., 25, 1163–1179, https://doi.org/10.1002/hyp.7644, 2011.

Folland, C. K., Knight, J., Linderholm, H. W., Fereday, D., Ineson, S., and Hurrell, J. W.: The Summer North Atlantic Oscillation: Past, Present, and Future, https://doi.org/10.1175/2008JCLI2459.1, 2009.

Freund, M. B., Helle, G., Balting, D. F., Ballis, N., Schleser, G. H., and Cubasch, U.: European tree-ring isotopes indicate unusual recent hydroclimate, Commun. Earth Environ., 4, 1–8, https://doi.org/10.1038/s43247-022-00648-7, 2023.

Gebrechorkos, S. H., Sheffield, J., Vicente-Serrano, S. M., Funk, C., Miralles, D. G., Peng, J., Dyer, E., Talib, J., Beck, H. E., Singer, M. B., and Dadson, S. J.: Warming accelerates global drought severity, Nature, 642, 628–635, https://doi.org/10.1038/s41586-025-09047-2, 2025.

Guha-Sapir, D., Hargitt, D., and Hoyois, P.: Thirty years of natural disasters 1974-2003: The numbers, Presses univ. de Louvain, ISBN: 2-930344-71-7, 2004.

Hamed, K. H.: Trend detection in hydrologic data: The Mann–Kendall trend test under the scaling hypothesis, J. Hydrol., 349, 350–363, https://doi.org/10.1016/j.jhydrol.2007.11.009, 2008.

Hamed, K. H. and Ramachandra Rao, A.: A modified Mann-Kendall trend test for autocorrelated data, J. Hydrol., 204, 182–196, https://doi.org/10.1016/S0022-1694(97)00125-X, 1998.

Hanel, M., Rakovec, O., Markonis, Y., Máca, P., Samaniego, L., Kyselý, J., and Kumar, R.: Revisiting the recent European droughts from a long-term perspective, Sci. Rep., 8, 9499, https://doi.org/10.1038/s41598-018-27464-4, 2018.

Hänsel, S.: Changes in the Characteristics of Dry and Wet Periods in Europe (1851–2015), Atmosphere, 11, 1080, https://doi.org/10.3390/atmos11101080, 2020.

Hänsel, S., Petzold, S., and Matschullat, J.: Precipitation Trend Analysis for Central Eastern Germany 1851–2006, in: Bioclimatology and Natural Hazards, edited by: Střelcová, K., Mátyás, C., Kleidon, A., Lapin, M., Matejka, F., Blaženec, M., Škvarenina, J., and Holécy, J., Springer Netherlands, Dordrecht, 29–38, https://doi.org/10.1007/978-1-4020-8876-6_3, 2009.

Hänsel, S., Ustrnul, Z., Łupikasza, E., and Skalak, P.: Assessing seasonal drought variations and trends over Central Europe, Adv. Water Resour., 127, 53–75, https://doi.org/10.1016/j.advwatres.2019.03.005, 2019.

Hänsel, S., Hoy, A., Brendel, C., and Maugeri, M.: Record summers in Europe: Variations in drought and heavy precipitation during 1901–2018, Int. J. Climatol., 42, 6235–6257, https://doi.org/10.1002/joc.7587, 2022.

van Haren, R., van Oldenborgh, G. J., Lenderink, G., Collins, M., and Hazeleger, W.: SST and circulation trend biases cause an underestimation of European precipitation trends, Clim. Dyn., 40, 1–20, https://doi.org/10.1007/s00382-012-1401-5, 2013.

Hartigan, J. A. and Wong, M. A.: Algorithm AS 136: A K-Means Clustering Algorithm, J. R. Stat. Soc. Ser. C Appl. Stat., 28, 100–108, https://doi.org/10.2307/2346830, 1979.

Hasanean, H. M., Almaashi, A. K., and Abdulhaleem H. Labban: Variability in Global Climatic Circulation Indices and Its Relationship, Atmosphere, 14, 1741, https://doi.org/10.3390/atmos14121741, 2023.

Haslinger, K. and Mayer, K.: Early spring droughts in Central Europe: Indications for atmospheric and oceanic drivers, Atmos. Sci. Lett., 24, e1136, https://doi.org/10.1002/asl.1136, 2023.

Haslinger, K., Hofstätter, M., Kroisleitner, C., Schöner, W., Laaha, G., Holawe, F., and Blöschl, G.: Disentangling Drivers of Meteorological Droughts in the European Greater Alpine Region During the Last Two Centuries, J. Geophys. Res. Atmos., 124, 12404–12425, https://doi.org/10.1029/2018JD029527, 2019.

Hernandez, A. and Comas-Bru, L.: East Atlantic and Scandinavian patterns, in: Atmospheric Oscillations, Elsevier, 183–202, https://doi.org/10.1016/B978-0-443-15638-0.00009-5, 2025.

Hoffmann, P. and Spekat, A.: Identification of possible dynamical drivers for long-term changes in temperature and rainfall patterns over Europe, Theor. Appl. Climatol., 143, 177–191, https://doi.org/10.1007/s00704-020-03373-3, 2021.

Hoover, D. L. and Smith, W. K.: The growing threat of multiyear droughts, Science, 387, 246–247, https://doi.org/10.1126/science.adu7419, 2025.

Huang, Y., Weis, J., Vereecken, H., and Hendricks Franssen, H.-J.: Long-term trends in agricultural droughts over Netherlands and Germany: how extreme was the year 2018?, Hydrol. Earth Syst. Sci. Discuss., 1–27, https://doi.org/10.5194/hess-2021-569, 2021.

Hurrell, J. W. and Van Loon, H.: Decadal Variations in Climate Associated with the North Atlantic Oscillation, in: Climatic Change at High Elevation Sites, edited by: Diaz, H. F., Beniston, M., and Bradley, R. S., Springer Netherlands, Dordrecht, 69–94, https://doi.org/10.1007/978-94-015-8905-5_4, 1997.

Huth, R., Beck, C., Philipp, A., Demuzere, M., Ustrnul, Z., Cahynová, M., Kyselý, J., and Tveito, O. E.: Classifications of Atmospheric Circulation Patterns: Recent Advances and Applications, Ann. N. Y. Acad. Sci., 1146, 105–152, https://doi.org/10.1196/annals.1446.019, 2008.

Ionita, M. and Nagavciuc, V.: Changes in drought features at the European level over the last 120 years, Nat. Hazards Earth Syst. Sci., 21, 1685–1701, https://doi.org/10.5194/nhess-21-1685-2021, 2021.

Ionita, M., Boroneanț, C., and Chelcea, S.: Seasonal modes of dryness and wetness variability over Europe and their connections with large scale atmospheric circulation and global sea surface temperature, Clim. Dyn., 45, 2803–2829, https://doi.org/10.1007/s00382-015-2508-2, 2015.

Ionita, M., Nagavciuc, V., Kumar, R., and Rakovec, O.: On the curious case of the recent decade, mid-spring precipitation deficit in central Europe, Npj Clim. Atmos. Sci., 3, 49, https://doi.org/10.1038/s41612-020-00153-8, 2020.

Ionita, M., Dima, M., Nagavciuc, V., Scholz, P., and Lohmann, G.: Past megadroughts in central Europe were longer, more severe and less warm than modern droughts, Commun. Earth Environ., 2, 61, https://doi.org/10.1038/s43247-021-00130-w, 2021.

IPCC: Annex III: Glossary [Planton, S.(Ed.)]. In: Climate Change 2013: The Physical Science Basis. Contribution of Working Group I to the Fifth Assessment Report of the Intergovernmental Panel on Climate Change [Stocker, TF, D. Qin, G.-K. Plattner, M. M. Tignor, S.K. Allen, J. Boschung, A. Nauels, Y. Xia, V. Bex and P.M. Midgley (eds.)]., Cambridge University Press., Cambridge, United Kingdom and New York, NY, USA, 2013.

Katerji, N. and Rana, G.: Crop Reference Evapotranspiration: A Discussion of the Concept, Analysis of the Process and Validation, Water Resour. Manag., 25, 1581–1600, https://doi.org/10.1007/s11269-010-9762-1, 2011.

Kautz, L.-A., Martius, O., Pfahl, S., Pinto, J. G., Ramos, A. M., Sousa, P. M., and Woollings, T.: Atmospheric blocking and weather extremes over the Euro-Atlantic sector – a review, Weather Clim. Dyn., 3, 305–336, https://doi.org/10.5194/wcd-3-305-2022, 2022.

Kendall, M. G.: Rank correlation methods, Griffin, Oxford, England, 1948.

Khaliq, M. N., Ouarda, T. B. M. J., Gachon, P., Sushama, L., and St-Hilaire, A.: Identification of hydrological trends in the presence of serial and cross correlations: A review of selected methods and their application to annual flow regimes of Canadian rivers, J. Hydrol., 368, 117–130, https://doi.org/10.1016/j.jhydrol.2009.01.035, 2009.

Kim, W. M., González-Rojí, S. J., and Raible, C. C.: Extratropical circulation associated with Mediterranean droughts during the Last Millennium in CMIP5 simulations, Clim. Past, 19, 2511–2533, https://doi.org/10.5194/cp-19-2511-2023, 2023.

Kingston, D. G., Stagge, J. H., Tallaksen, L. M., and Hannah, D. M.: European-Scale Drought: Understanding Connections between Atmospheric Circulation and Meteorological Drought Indices, https://doi.org/10.1175/JCLI-D-14-00001.1, 2015.

KNMI Climate Explorer: de Bilt: Koninklijk Nederlands Meteorologisch Instituut (KNMI), https://climexp.knmi.nl/start.cgi, 2022.

Lekarkar, K., Rakovec, O., Kumar, R., Dondeyne, S., and van Griensven, A.: Reconstructed soil moisture droughts in Belgium reveal 2011–2020 was the driest decade since 1970, Hydrol. Earth Syst. Sci., 30, 2817–2835, https://doi.org/10.5194/hess-30-2817-2026, 2026.

Lenderink, G., van Meijgaard, E., and Selten, F.: Intense coastal rainfall in the Netherlands in response to high sea surface temperatures: analysis of the event of August 2006 from the perspective of a changing climate, Clim. Dyn., 32, 19–33, https://doi.org/10.1007/s00382-008-0366-x, 2009.

Lhotka, O., Trnka, M., Kyselý, J., Markonis, Y., Balek, J., and Možný, M.: Atmospheric Circulation as a Factor Contributing to Increasing Drought Severity in Central Europe, J. Geophys. Res. Atmos., 125, e2019JD032269, https://doi.org/10.1029/2019JD032269, 2020.

Lloyd-Hughes, B.: The impracticality of a universal drought definition, Theor. Appl. Climatol., 117, 607–611, https://doi.org/10.1007/s00704-013-1025-7, 2014.

Mann, H. B.: Nonparametric Tests Against Trend, Econometrica, 13, 245–259, https://doi.org/10.2307/1907187, 1945.

Maslin, M., Ramnath, R. D., Welsh, G. I., and Sisodiya, S. M.: Understanding the health impacts of the climate crisis, Future Healthc. J., 12, 100240, https://doi.org/10.1016/j.fhj.2025.100240, 2025.

Matthews, B. W.: Comparison of the predicted and observed secondary structure of T4 phage lysozyme, Biochim. Biophys. Acta BBA - Protein Struct., 405, 442–451, https://doi.org/https://doi.org/10.1016/0005-2795(75)90109-9, 1975.

McKee, T. B., Doesken, N. J., Kleist, J., and others: The relationship of drought frequency and duration to time scales, in: Proceedings of the 8th Conference on Applied Climatology, 179–183, 1993.

Mens, M. J. P., van Rhee, G., Schasfoort, F., and Kielen, N.: Integrated drought risk assessment to support adaptive policymaking in the Netherlands, Nat. Hazards Earth Syst. Sci., 22, 1763–1776, https://doi.org/10.5194/nhess-22-1763-2022, 2022.

Miralles, D. G., Gentine, P., Seneviratne, S. I., and Teuling, A. J.: Land–atmospheric feedbacks during droughts and heatwaves: state of the science and current challenges, Ann. N. Y. Acad. Sci., 1436, 19–35, https://doi.org/10.1111/nyas.13912, 2019.

Moberg, A. and Jones, P. D.: Trends in indices for extremes in daily temperature and precipitation in central and western Europe, 1901-99, Int. J. Climatol., 25, 1149–1171, https://doi.org/10.1002/joc.1163, 2005.

van Mourik, J., Ruijsch, D., van der Wiel, K., Hazeleger, W., and Wanders, N.: Regional drivers and characteristics of multi-year droughts, Weather Clim. Extrem., 48, 100748, https://doi.org/10.1016/j.wace.2025.100748, 2025.

Obasi, G.: WMO's role in the international decade for natural disaster reduction, Bull. Am. Meteorol. Soc., 75, 1655–1661, https://www.jstor.org/stable/26231968, 1994.

Oikonomou, P. D., Karavitis, C. A., Tsesmelis, D. E., Kolokytha, E., and Maia, R.: Drought Characteristics Assessment in Europe over the Past 50 Years, Water Resour. Manag., 34, 4757–4772, https://doi.org/10.1007/s11269-020-02688-0, 2020.

Patakamuri, S. K. and O'Brien, N.: modifiedmk: Modified Versions of Mann Kendall and Spearman's Rho Trend Tests, https://doi.org/10.32614/CRAN.package.modifiedmk, 2017.

Pauling, A., Luterbacher, J., Casty, C., and Wanner, H.: Five hundred years of gridded high-resolution precipitation reconstructions over Europe and the connection to large-scale circulation, Clim. Dyn., 26, 387–405, https://doi.org/10.1007/s00382-005-0090-8, 2006.

Penman, H. L.: Natural evaporation from open water, bare soil and grass, Proc. R. Soc. Lond. Math. Phys. Sci., 193, 120–145, https://doi.org/10.1098/rspa.1948.0037, 1948.

Pfister, L., Wilhelm, L., Brugnara, Y., Imfeld, N., and Brönnimann, S.: Weather type reconstruction using machine learning approaches, Weather Clim. Dyn., 6, 571–594, https://doi.org/10.5194/wcd-6-571-2025, 2025.

Philip, S. Y., Kew, S. F., van der Wiel, K., Wanders, N., and Jan van Oldenborgh, G.: Regional differentiation in climate change induced drought trends in the Netherlands, Environ. Res. Lett., 15, 094081, https://doi.org/10.1088/1748-9326/ab97ca, 2020.

Philipp, A., Della-Marta, P. M., Jacobeit, J., Fereday, D. R., Jones, P. D., Moberg, A., and Wanner, H.: Long-Term Variability of Daily North Atlantic–European Pressure Patterns since 1850 Classified by Simulated Annealing Clustering, https://doi.org/10.1175/JCLI4175.1, 2007.

R Core Team: R: A language and environment for statistical computing, R Found. Stat. Comput. Vienna Austria, 2021.

Raible, C. C., Bärenbold, O., and Gómez-navarro, J. J.: Drought indices revisited – improving and testing of drought indices in a simulation of the last two millennia for Europe, Tellus Dyn. Meteorol. Oceanogr., 69, 1287492, https://doi.org/10.1080/16000870.2017.1296226, 2017.

Raposo, V. D. M. B., Costa, V. A. F., and Rodrigues, A. F.: A review of recent developments on drought characterization, propagation, and influential factors, Sci. Total Environ., 898, 165550, https://doi.org/10.1016/j.scitotenv.2023.165550, 2023.

Rousi, E., Selten, F., Rahmstorf, S., and Coumou, D.: Changes in North Atlantic Atmospheric Circulation in a Warmer Climate Favor Winter Flooding and Summer Drought over Europe, J. Clim., 34, 2277–2295, https://doi.org/10.1175/JCLI-D-20-0311.1, 2021.

Ruijsch, D., van Mourik, J., Biemans, H., Hauswirth, S. M., and Wanders, N.: Thrive or Wither: Exploring the Impacts of Multiyear Droughts on Vegetation, J. Geophys. Res. Biogeosciences, 130, e2025JG008992, https://doi.org/10.1029/2025JG008992, 2025.

Savary, O., Ardilouze, C., and Cattiaux, J.: Linking European droughts to year-round weather regimes, Weather Clim. Dyn., 7, 223–245, https://doi.org/10.5194/wcd-7-223-2026, 2026.

van der Schrier, G., Briffa, K. R., Jones, P. D., and Osborn, T. J.: Summer Moisture Variability across Europe, J. Clim., 19, 2818–2834, https://doi.org/10.1175/JCLI3734.1, 2006.

van der Schrier, G., Allan, R. P., Ossó, A., Sousa, P. M., Van de Vyver, H., Van Schaeybroeck, B., Coscarelli, R., Pasqua, A. A., Petrucci, O., Curley, M., Mietus, M., Filipiak, J., Štěpánek, P., Zahradníček, P., Brázdil, R., Řezníčková, L., van den Besselaar, E. J. M., Trigo, R., and Aguilar, E.: The 1921 European drought: impacts, reconstruction and drivers, Clim. Past, 17, 2201–2221, https://doi.org/10.5194/cp-17-2201-2021, 2021.

Schwander, M., Rohrer, M., Brönnimann, S., and Malik, A.: Influence of solar variability on the occurrence of central European weather types from 1763 to 2009, Clim. Past, 13, 1199–1212, https://doi.org/10.5194/cp-13-1199-2017, 2017.

Sen, P. K.: Estimates of the Regression Coefficient Based on Kendall's Tau, J. Am. Stat. Assoc., 63, 1379–1389, https://doi.org/10.1080/01621459.1968.10480934, 1968.

Seneviratne, S. I.: Historical drought trends revisited, Nature, 491, 338–339, https://doi.org/10.1038/491338a, 2012.

Seneviratne, S. I., Lüthi, D., Litschi, M., and Schär, C.: Land–atmosphere coupling and climate change in Europe, Nature, 443, 205–209, https://doi.org/10.1038/nature05095, 2006.

Serras, F., Vandelanotte, K., Borgers, R., Van Schaeybroeck, B., Termonia, P., Demuzere, M., and van Lipzig, N. P. M.: Optimizing climate model selection in regional studies using an adaptive weather type based framework: a case study for extreme heat in Belgium, Clim. Dyn., 62, 9927–9949, https://doi.org/10.1007/s00382-024-07432-7, 2024.

Sheffield, J., Wood, E. F., and Roderick, M. L.: Little change in global drought over the past 60 years, Nature, 491, 435–438, https://doi.org/10.1038/nature11575, 2012.

Simpson, I., Hanna, E., Baker, L., Sun, Y., and Wei, H.-L.: North Atlantic atmospheric circulation indices: Links with summer and winter temperature and precipitation in north-west Europe, including persistence and variability, Int. J. Climatol., 44, 902–922, https://doi.org/10.1002/joc.8364, 2024.

Slivinski, L. C.: Historical Reanalysis: What, How, and Why?, J. Adv. Model. Earth Syst., 10, 1736–1739, https://doi.org/10.1029/2018MS001434, 2018.

Slivinski, L. C., Compo, G. P., Whitaker, J. S., Sardeshmukh, P. D., Giese, B. S., McColl, C., Allan, R., Yin, X., Vose, R., Titchner, H., Kennedy, J., Spencer, L. J., Ashcroft, L., Brönnimann, S., Brunet, M., Camuffo, D., Cornes, R., Cram, T. A., Crouthamel, R., Domínguez-Castro, F., Freeman, J. E., Gergis, J., Hawkins, E., Jones, P. D., Jourdain, S., Kaplan, A., Kubota, H., Blancq, F. L., Lee, T.-C., Lorrey, A., Luterbacher, J., Maugeri, M., Mock, C. J., Moore, G. W. K., Przybylak, R., Pudmenzky, C., Reason, C., Slonosky, V. C., Smith, C. A., Tinz, B., Trewin, B., Valente, M. A., Wang, X. L., Wilkinson, C., Wood, K., and Wyszyński, P.: Towards a more reliable historical reanalysis: Improvements for version 3 of the Twentieth Century Reanalysis system, Q. J. R. Meteorol. Soc., 145, 2876–2908, https://doi.org/10.1002/qj.3598, 2019.

Slivinski, L. C., Compo, G. P., Sardeshmukh, P. D., Whitaker, J. S., McColl, C., Allan, R. J., Brohan, P., Yin, X., Smith, C. A., Spencer, L. J., Vose, R. S., Rohrer, M., Conroy, R. P., Schuster, D. C., Kennedy, J. J., Ashcroft, L., Brönnimann, S., Brunet, M., Camuffo, D., Cornes, R., Cram, T. A., Domínguez-Castro, F., Freeman, J. E., Gergis, J., Hawkins, E., Jones, P. D., Kubota, H., Lee, T. C., Lorrey, A. M., Luterbacher, J., Mock, C. J., Przybylak, R. K., Pudmenzky, C., Slonosky, V. C., Tinz, B., Trewin, B., Wang, X. L., Wilkinson, C., Wood, K., and Wyszyński, P.: An Evaluation of the Performance of the Twentieth Century Reanalysis Version 3, https://doi.org/10.1175/JCLI-D-20-0505.1, 2021.

Soci, C., Hersbach, H., Simmons, A., Poli, P., Bell, B., Berrisford, P., Horányi, A., Muñoz-Sabater, J., Nicolas, J., Radu, R., Schepers, D., Villaume, S., Haimberger, L., Woollen, J., Buontempo, C., and Thépaut, J.-N.: The ERA5 global reanalysis from 1940 to 2022, Q. J. R. Meteorol. Soc., 150, 4014–4048, https://doi.org/10.1002/qj.4803, 2024.

Spinoni, J., Naumann, G., Carrao, H., Barbosa, P., and Vogt, J.: World drought frequency, duration, and severity for 1951–2010, Int. J. Climatol., 34, 2792–2804, https://doi.org/10.1002/joc.3875, 2014.

Spinoni, J., Naumann, G., Vogt, J., and Barbosa, P.: European drought climatologies and trends based on a multi-indicator approach, Glob. Planet. Change, 127, 50–57, https://doi.org/10.1016/j.gloplacha.2015.01.012, 2015.

Spinoni, J., Naumann, G., Vogt, J., and Barbosa, P.: Meteorological Droughts in Europe: Events and Impacts: Past Trends and Future Projections, https://doi.org/10.2788/79637, 2016.

Spinoni, J., Naumann, G., and Vogt, J. V.: Pan-European seasonal trends and recent changes of drought frequency and severity, Glob. Planet. Change, 148, 113–130, https://doi.org/10.1016/j.gloplacha.2016.11.013, 2017.

Spinoni, J., Vogt, J. V., Naumann, G., Barbosa, P., and Dosio, A.: Will drought events become more frequent and severe in Europe?, Int. J. Climatol., 38, 1718–1736, https://doi.org/10.1002/joc.5291, 2018.

Spinoni, J., Barbosa, P., De Jager, A., McCormick, N., Naumann, G., Vogt, J. V., Magni, D., Masante, D., and Mazzeschi, M.: A new global database of meteorological drought events from 1951 to 2016, J. Hydrol. Reg. Stud., 22, 100593, https://doi.org/10.1016/j.ejrh.2019.100593, 2019.

Stagge, J. H., Tallaksen, L. M., Gudmundsson, L., Van Loon, A. F., and Stahl, K.: Candidate Distributions for Climatological Drought Indices (SPI and SPEI), Int. J. Climatol., 35, 4027–4040, https://doi.org/10.1002/joc.4267, 2015.

Stahl, K. and Demuth, S.: Linking streamflow drought to the occurrence of atmospheric circulation patterns, Hydrol. Sci. J., 44, 467–482, https://doi.org/10.1080/02626669909492240, 1999.

Stahl, K., Kohn, I., Blauhut, V., Urquijo, J., De Stefano, L., Acácio, V., Dias, S., Stagge, J. H., Tallaksen, L. M., Kampragou, E., Van Loon, A. F., Barker, L. J., Melsen, L. A., Bifulco, C., Musolino, D., de Carli, A., Massarutto, A., Assimacopoulos, D., and Van Lanen, H. A. J.: Impacts of European drought events: insights from an international database of text-based reports, Nat. Hazards Earth Syst. Sci., 16, 801–819, https://doi.org/10.5194/nhess-16-801-2016, 2016.

Stefanon, M., D'Andrea, F., and Drobinski, P.: Heatwave classification over Europe and the Mediterranean region, Environ. Res. Lett., 7, 014023, https://doi.org/10.1088/1748-9326/7/1/014023, 2012.

Stegehuis, A. I., Vogel, M. M., Vautard, R., Ciais, P., Teuling, A. J., and Seneviratne, S. I.: Early Summer Soil Moisture Contribution to Western European Summer Warming, J. Geophys. Res. Atmos., 126, e2021JD034646, https://doi.org/10.1029/2021JD034646, 2021.

Suarez-Gutierrez, L., Müller, W. A., Li, C., and Marotzke, J.: Dynamical and thermodynamical drivers of variability in European summer heat extremes, Clim. Dyn., 54, 4351–4366, https://doi.org/10.1007/s00382-020-05233-2, 2020.

Svensson, C. and Hannaford, J.: Oceanic conditions associated with Euro-Atlantic high pressure and UK drought, Environ. Res. Commun., 1, 101001, https://doi.org/10.1088/2515-7620/ab42f7, 2019.

Tapia, C., Abajo, B., Feliu, E., Mendizabal, M., Martinez, J. A., Fernández, J. G., Laburu, T., and Lejarazu, A.: Profiling urban vulnerabilities to climate change: An indicator-based vulnerability assessment for European cities, Ecol. Indic., 78, 142–155, https://doi.org/10.1016/j.ecolind.2017.02.040, 2017.

Thornthwaite, C. W.: An Approach toward a Rational Classification of Climate, Geogr. Rev., 38, 55–94, https://doi.org/10.2307/210739, 1948.

Tomas-Burguera, M., Vicente-Serrano, S. M., Peña-Angulo, D., Domínguez-Castro, F., Noguera, I., and El Kenawy, A.: Global Characterization of the Varying Responses of the Standardized Precipitation Evapotranspiration Index to Atmospheric Evaporative Demand, J. Geophys. Res. Atmos., 125, e2020JD033017, https://doi.org/10.1029/2020JD033017, 2020.

Topál, D., Herein, M., and Haszpra, T.: Northern Annular Mode, in: Atmospheric Oscillations, Elsevier, 203–219, https://doi.org/10.1016/B978-0-443-15638-0.00010-1, 2025.

Trenberth, K. E., Dai, A., van der Schrier, G., Jones, P. D., Barichivich, J., Briffa, K. R., and Sheffield, J.: Global warming and changes in drought, Nat. Clim. Change, 4, 17–22, https://doi.org/10.1038/nclimate2067, 2014.

Trnka, M., Kyselý, J., Možný, M., and Dubrovský, M.: Changes in Central-European soil-moisture availability and circulation patterns in 1881–2005, Int. J. Climatol., 29, 655–672, https://doi.org/10.1002/joc.1703, 2009.

Tuel, A. and Eltahir, E. A. B.: Mechanisms of European Summer Drying under Climate Change, https://doi.org/10.1175/JCLI-D-20-0968.1, 2021.

Valler, V., Franke, J., Brugnara, Y., Burgdorf, A.-M., Lundstad, E., Hand, R., Samakinwa, E., Lipfert, L., Friedman, A. R., and Brönnimann, S.: ModE-RA - A global monthly paleo-reanalysis of the modern era (1421 to 2008): Set 1420-3_1850-1, https://doi.org/10.26050/WDCC/ModE-RA_s14203-18501, 2023.

Valler, V., Franke, J., Brugnara, Y., Samakinwa, E., Hand, R., Lundstad, E., Burgdorf, A.-M., Lipfert, L., Friedman, A. R., and Brönnimann, S.: ModE-RA: a global monthly paleo-reanalysis of the modern era 1421 to 2008, Sci. Data, 11, 36, https://doi.org/10.1038/s41597-023-02733-8, 2024.

Van Oldenborgh, G. J., Burgers, G., and Tank, A. K.: On the El Niño teleconnection to spring precipitation in Europe, Int. J. Climatol., 20, 565–574, https://doi.org/10.1002/(SICI)1097-0088(200004)20:5%3C565::AID-JOC488%3E3.0.CO;2-5, 2000.

Vicente-Serrano, S. M. and López-Moreno, J. I.: Nonstationary influence of the North Atlantic Oscillation on European precipitation, J. Geophys. Res. Atmos., 113, https://doi.org/10.1029/2008JD010382, 2008.

Vicente-Serrano, S. M., Beguería, S., and López-Moreno, J. I.: A Multiscalar Drought Index Sensitive to Global Warming: The Standardized Precipitation Evapotranspiration Index, J. Clim., 23, 1696–1718, https://doi.org/10.1175/2009JCLI2909.1, 2010.

Vicente-Serrano, S. M., Domínguez-Castro, F., Murphy, C., Hannaford, J., Reig, F., Peña-Angulo, D., Tramblay, Y., Trigo, R. M., Mac Donald, N., Luna, M. Y., Mc Carthy, M., Van der Schrier, G., Turco, M., Camuffo, D., Noguera, I., García-Herrera, R., Becherini, F., Della Valle, A., Tomas-Burguera, M., and El Kenawy, A.: Long-term variability and trends in meteorological droughts in Western Europe (1851–2018), Int. J. Climatol., 41, https://doi.org/10.1002/joc.6719, 2021.

Vicente-Serrano, S. M., Peña-Angulo, D., Beguería, S., Domínguez-Castro, F., Tomás-Burguera, M., Noguera, I., Gimeno-Sotelo, L., and El Kenawy, A.: Global drought trends and future projections, Philos. Trans. R. Soc. Math. Phys. Eng. Sci., 380, 20210285, https://doi.org/10.1098/rsta.2021.0285, 2022.

Villani, L., Piemontese, L., Castelli, G., Borgo, A., Ghilain, N., Van Schaeybroeck, B., Lucca, E., Aslam, M. F., Debolini, M., Bouizrou, I., Yimer, E. A., Baudewyn, M., Jaramillo, F., Trabucco, A., van Griensven, A., Penna, D., and Bresci, E.: Neglecting plant physiology: systematic overestimation of drought projections, Environ. Res. Clim., https://doi.org/10.1088/2752-5295/ae583c, 2026.

Visbeck, M. H., Hurrell, J. W., Polvani, L., and Cullen, H. M.: The North Atlantic Oscillation: Past, present, and future, Proc. Natl. Acad. Sci. U. S. A., 98, 12876–12877, https://doi.org/10.1073/pnas.231391598, 2001.

Vogel, E., Donat, M. G., Alexander, L. V., Meinshausen, M., Ray, D. K., Karoly, D., Meinshausen, N., and Frieler, K.: The effects of climate extremes on global agricultural yields, Environ. Res. Lett., 14, 054010, https://doi.org/10.1088/1748-9326/ab154b, 2019.

Wang, Y., Rammig, A., Blickensdörfer, L., Wang, Y., Zhu, X. X., and Buras, A.: Species-specific responses of canopy greenness to the extreme droughts of 2018 and 2022 for four abundant tree species in Germany, Sci. Total Environ., 958, 177938, https://doi.org/10.1016/j.scitotenv.2024.177938, 2025.

van der Wiel, K., Lenderink, G., and de Vries, H.: Physical storylines of future European drought events like 2018 based on ensemble climate modelling, Weather Clim. Extrem., 33, 100350, https://doi.org/10.1016/j.wace.2021.100350, 2021.

van der Wiel, K., Batelaan, T. J., and Wanders, N.: Large increases of multi-year droughts in north-western Europe in a warmer climate, Clim. Dyn., 60, 1781–1800, https://doi.org/10.1007/s00382-022-06373-3, 2023.

World Meteorological Organization: Standardized precipitation index: user guide (M. Svoboda, M. Hayes and D. Wood), WMO-No 1090 Geneva, 2012.

WorldPop: Global 1km Population, , https://doi.org/10.5258/SOTON/WP00647, 2018.

Xue, H., Goosse, H., Dalaiden, Q., Seftigen, K., Gennaretti, F., and Shi, F.: Scandinavian pattern and temperature changes shape European summer droughts over the past millennium, Nat. Commun., https://doi.org/10.1038/s41467-026-72385-w, 2026.

Yin, Z., Dong, B., Wei, W., and Yang, S.: Anthropogenic Impacts on Amplified Midlatitude European Summer Warming and Rapid Increase of Heatwaves in Recent Decades, Geophys. Res. Lett., 51, e2024GL108982, https://doi.org/10.1029/2024GL108982, 2024.

Zanaga, D., Van De Kerchove, R., Daems, D., De Keersmaecker, W., Brockmann, C., Kirches, G., Wevers, J., Cartus, O., Santoro, M., Fritz, S., and others: ESA WorldCover 10 m 2021 v200, https://doi.org/10.5281/zenodo.7254221, 2022.

Zscheischler, J. and Fischer, E. M.: The record-breaking compound hot and dry 2018 growing season in Germany, Weather Clim. Extrem., 29, 100270, https://doi.org/10.1016/j.wace.2020.100270, 2020.

Zscheischler, J., Martius, O., Westra, S., Bevacqua, E., Raymond, C., Horton, R. M., van den Hurk, B., AghaKouchak, A., Jézéquel, A., Mahecha, M. D., Maraun, D., Ramos, A. M., Ridder, N. N., Thiery, W., and Vignotto, E.: A typology of compound weather and climate events, Nat. Rev. Earth Environ., 1, 333–347, https://doi.org/10.1038/s43017-020-0060-z, 2020.